

THE INFLUENCE OF  
POLYMER CONCENTRATION, SOLVENT AND SPINNING TEMPERATURE  
ON PVDF FIBER CRYSTALLINITY AND CRYSTALLINE PHASE FORMATION

A Thesis

Presented to the Faculty of the Graduate School

of Cornell University

In Partial Fulfillment of the Requirements for the Degree of

Master of Science

by

Sun Young Park

August 2012

© 2012 Sun Young Park

## ABSTRACT

PVDF nanofibers were electrospun from solution in dimethylacetamide (DMAC)/ acetone mixed solvent at temperatures ranging from 25 °C to 55 °C with a goal of maximizing the  $\beta$  crystalline phase which has piezoelectric properties. Between 12 and 18wt% of Poly (vinylidene fluoride) (PVDF) was dissolved in the solvent(14v% to 50v%) and nonsolvent mixture(50v% to 86v%). The solvent capable of dissolving PVDF pellets is DMAc and the acetone is latent solvent which requires high temperature to dissolve PVDF. Acetone which has high volatility was added to improve the electrospinning process by changing viscosity of solution and evaporation of solvent. Its effect on viscosity and evaporation influenced by the polymer concentration and the spinning temperature is responsible to produce different fiber morphology and crystalline phases. Fiber diameter ranges from 0.1 to 3.6 $\mu$ m. Smallest fibers are found when the spinning solution combines lower PVDF concentration as 12 or 14wt% and higher volume percent of acetone, 83 or 86v%, regardless of spinning temperature. Although finest fibers with best fiber morphology are found at high volume percent of acetone, those fibers do not possess high % $\beta$  crystallinity as there is no correlation between fiber morphology and the crystallinity. However, those fibers which exhibit high % $\beta$  crystallinity also present uniform fibers without residual solvent or beads. Obtained by XRD, %total crystallinity and % $\beta$  crystallinity have correlation so fibers with high crystallinity could have high piezoelectric properties. Total crystallinity

measured by XRD has a maximum of 52% when the fibers are spun from the solution of 12wt%PVDF and solvent of 80v%acetone and 20v%DMAc at 55°C. The same solution produces the fibers with maximum  $\beta$  crystallinity 35%. The maximum 35%  $\beta$  crystallinity is also achieved under other spinning conditions. Analyzing XRD results from different composition concludes that there are many ways to increase % $\beta$  crystallinity. Investigating combined effect of acetone and concentration at different spinning temperature shows significantly varying results at different temperature. At different temperature, % $\beta$  crystallinity correspond differently to the combined effect and the simplest way is to use spinning temperature of 55°C with 80v%acetone in the solvent. With this combination, many concentrations can maximize % $\beta$  crystallinity. %Total crystallinity was also investigated by DSC although there is no correlation with the data from XRD. Heat flow shows large cold crystallization peak for solution with low volume percent of acetone. This states that fibers from those solutions were not able to crystallize fully during the electrospinning process. For better understanding of spinning, rheometer was used. The study proves that the influence of the acetone on both viscosity and evaporation. The comparison with fiber morphology points the limitation of acetone to decrease viscosity on concentration and the limitation of concentration to slow evaporation rate on the volume percent of acetone. The rheology also indicates the link between spinnable condition and chain entanglement measured by storage modulus. While interaction between three variables creates complication to identify the conditions to maximize % $\beta$

crystallinity, also investigating many factors suggests several ways to improve formation of  $\beta$  crystallinity. Few conditions have been located to produce fibers with high piezoelectric properties and these conditions also produce good fiber morphology.  $\beta$  crystallinity of these fibers can be increased further using other methods and the uniform fibers with the high piezoelectric properties can be applied in many ways.

## BIOGRAPHICAL SKETCH

Sun Young Park, born July 1986, grew up in Busan, South Korea. She graduated from Oldfields School (2005) located near Baltimore, Maryland and Carnegie Mellon University (2009) with a Bachelor of Science degree in Materials Science and Engineering and minor in Business Administration.

## ACKNOWLEDGMENTS

Great appreciation to Dr. Margaret Frey and Dr. Yong L. Joo for advice and encouragement and to Frey's research group/writing group for suggestions and support

## TABLE OF CONTENTS

Biographical Sketch-----	iii
Acknowledgements-----	iv
CHAPTER 1: INTRODUCTION-----	1
CHAPTER 2: LITERATURE REVIEW-----	4
2.1 Poly(vinylidene fluoride)-----	4
2.1.1 Applications -----	5
2.1.2 Electrical Properties-----	6
2.2 Crystallinity-----	6
2.3 Piezoelectricity-----	9
2.4 Solvent-Non-solvent System-----	11
2.5 Electrospinning-----	13
CHAPTER 3: EXPERIMENTAL APPROACH-----	18
3.1 Materials-----	18
3.2 Instruments-----	18
3.3 Experimental Procedures-----	19
3.3.1 Electrospinning Experiments-----	19
3.3.2 Rheological Experiments-----	20
3.3.3 SEM Image Analysis-----	21
3.3.4 %Crystallinity from DSC-----	22
3.3.5 %Crystallinity from XRD-----	22
3.3.6 Statistical Analysis-----	22
CHAPTER 4: RESULTS AND DISCUSSION-----	23
4.1 Electrospinning -----	24
4.2 Rheological Analysis-----	24
4.3 Fiber Morphology-----	34
4.4 Crystallinity and Crystalline phases-----	52
4.5 Statistical Analysis-----	67
CHAPTER 5: CONCLUSIONS-----	73
CHAPTER 6: FUTURE WORK-----	75
APPENDIX A: DSC Data of Electrospun PVDF Fibers-----	76
APPENDIX B: XRD Data of Electrospun PVDF Fibers-----	78
REFERENCES-----	80

## CHAPTER 1

### INTRODUCTION

Polyvinylidene fluoride (PVDF) is the only polymer that demonstrates strong and stable piezoelectric properties. PVDF has a semi-crystalline structure which has both crystalline and amorphous regions and the crystalline regions distributed within an amorphous matrix. There are four,  $\alpha$ (II),  $\beta$ (I),  $\gamma$ (III),  $\delta$ (IV,IIp), or possibly more types of crystalline polymorphs. PVDF polymer chains consist of a carbon backbone with every other carbon atom bonded to pairs of hydrogen atoms or pairs of fluorine atoms. Polymerization of  $-\text{CH}_2-\text{CF}_2-$  was first discovered in 1944. Hydrogen atoms are electropositive and fluorine atoms are electronegative.  $\alpha$ , anti-parallel conformation, and  $\beta$ , transverse conformation, are the most common crystalline phases of PVDF chain.  $\alpha$  phase is found commonly and it is non-polar molecule that creates no net dipole and hence no piezoelectric effect. The  $\beta$  phase, which does exhibit the piezoelectric effect, is less common. When PVDF chains are crystallized in the piezoelectric  $\beta$  phase, all hydrogen atoms are move to one side and fluorine to opposite side. When mechanical stress is applied to the  $\beta$  phase, hydrogen and fluorine atoms shift relative to each other and generate an electric dipole and field. In order to have power generation property, fibers must have  $\beta$  phase PVDF crystals. Electrospinning is a simple method for drawing polymer fibers with diameters at nano or micron scale using high voltage supply. Electrospun fibers are

semicrystalline and have characteristics of high porosity, small diameter, excellent pore interconnectivity and high surface to volume ratio. Also, electrospun fibers can be uniaxially aligned over long length in centimeter scale. The products vary with temperature, feeding rate, applied voltage, diameter of the needle, distance between the needle tip and the ground and the conductivity of the collector. Fibers also depend on the viscosity, conductivity and surface tension of the solution resulted from polymer type and its molecular weight, concentration of the solution and solvent composition and its evaporation rate.

Electrospinning is a technique to produce piezoelectric  $\beta$  phase PVDF fibers by the mechanical force of drawing. However, when the molecular chains are not highly aligned relative to each other, the fibers will not have piezoelectric property. Electrospinning forms a fiber by buildup of charge at the surface of the polymer solution droplet to push towards a grounded substrate. If the voltage creates the force greater enough to overcome the surface tension, droplet, called the Taylor cone, becomes thin jet. This jet with whipping instability accelerates as it gets closer to the ground. When the viscosity of the solution controlled by the concentration is adequate, the jet becomes stable. Before jet reaches the ground, the polymer solution is stretched due to the electric field applied and the solvent evaporates. This process results in ultrathin fibers and formed as a randomly oriented pile of nonwoven fibers on the collector.

Non-solvent can be added in the solution to help the electrospinning process. Acetone impedes the formation of droplets and improves homogeneity. While acetone makes the solution less viscous, it has high volatility. While acetone can lower the spinnable concentration, it can also affect the crystalline phase formation. Lower evaporation temperature helps to decrease the amount of  $\alpha$  phase and  $\beta$  phase preferably formed with lower evaporation rate and  $\alpha$  phase with higher rate.

PVDF fibers can be stressed mechanically in either the longitudinal or transverse mode but the transverse direction is more convenient for power generation because it allows placement of electrodes along the length of the fiber. PVDF has high a piezoelectric coefficient which allows it to endure large strain and it also has bio compatibility and low acoustic and mechanical impedance. Fibers which generate electric charge can be produced using PVDF and can be incorporated into sails, garments, flags, wind socks, upholstery, draperies or tents to generate power from textile objects during their normal use.

## CHAPTER 2

### LITERATURE REVIEW

#### 2.1 Poly(vinylidene fluoride)

Polymerization of  $-\text{CH}_2\text{-CF}_2-$  was first discovered in 1944<sup>1</sup>. In 1969, Kawai calculated the piezoelectric coefficient of thin film of poled PVDF after applying an electric field and it was ten times larger than that of the other polymers. Twenty years later, Barsky et al. developed a sensor feedback using PVDF and the microgripper system was improved in 2003.<sup>2</sup> PVDF polymer chains consist of a carbon backbone with every other carbon atom bonded to pairs of hydrogen atoms or pairs of fluorine atoms. In the structure of PVDF shown in Figure 2.1.1, hydrogen atoms are electropositive and fluorine atoms are electronegative.

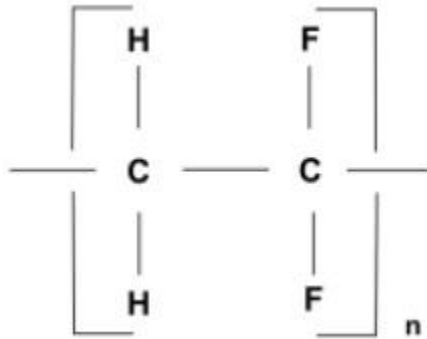


Figure 2.1. 1 Structure of PVDF

The monomeric unit of PVDF has a directionality of head( $\text{CH}_2$ ) and tail( $\text{CF}_2$ ) and that causes structural irregularity of head-to-head and tail-to-tail linkage of monomers. This affects the structural stability of the crystal polymorphs.<sup>3</sup>

PVDF has a glass transition temperature at  $-40^{\circ}\text{C}$  and the melting point is  $175^{\circ}\text{C}$ . PVDF can also be processed into fibers. Fibers can be stressed mechanically in either the longitudinal or transverse mode but the transverse direction is more convenient for power generation because it allows placement of electrodes along the length of the fiber. PVDF has high a piezoelectric coefficient which allows it to endure large strain and it also has bio compatibility and low acoustic and mechanical impedance. <sup>4</sup>

### **2.1.1 Applications**

PVDF has various applications due to its exceptional mechanical strength, excellent resistance to abrasion, deformation, creep and fatigue. Its high crystalline fraction, about 50%, and resistance to chemicals and sunlight allows more wide application <sup>1</sup>. Also, while it is less expensive than other ceramic piezoelectric materials, it has wider applications than brittle ceramic piezoelectric. <sup>5</sup> Fibers which generate electric charge can be produced using PVDF and can be incorporated into sails, garments, flags, wind socks, upholstery, draperies or tents to generate power from textile objects during their normal use.

### **2.1.2 Electrical Properties**

Ferroelectric property of PVDF is first discovered in early 1970s while investigating electrets. It is a macroscopic separation of positive and negative

charges by applying an electric field orienting permanent dipoles or creating a space charge by injecting free charges. Ferroelectric is a change of direction in polar unit cell in crystalline material when the electric field is applied.

Polarization by orienting dipoles which though may not be in crystalline phase or space charge in polymer which has homogeneous mechanical property causes piezoelectricity. <sup>1</sup>

## 2.2 Crystallinity

PVDF has a semi-crystalline structure which has both crystalline and amorphous regions and the crystalline regions distributed within an amorphous matrix. <sup>6</sup> There are four,  $\alpha$ (II),  $\beta$ (I),  $\gamma$ (III),  $\delta$ (IV,IIp), or possibly more types of crystalline polymorphs. The  $\alpha$  crystal form is most common, however, the  $\beta$  crystal form has unique paramagnetic and piezoelectric properties.

Figure 2.2.1 shows different ways to produce each crystalline form and figure 2.2.2 shows each crystalline structure.

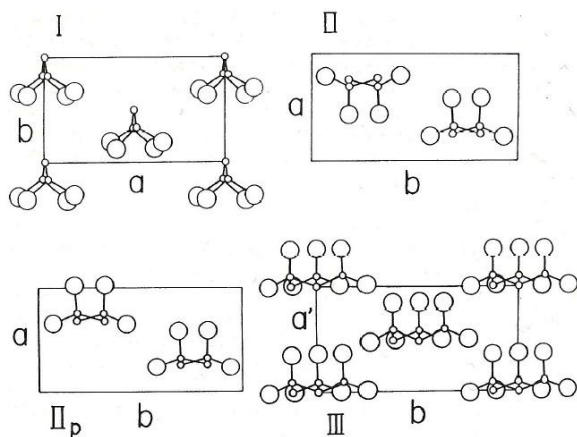


Figure 2.2. 1 Crystal Structure of four crystalline modification of PVDF

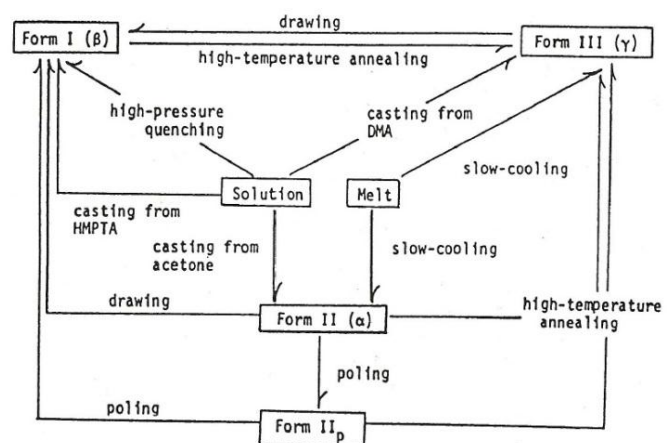


Figure 2.2. 2 Interconversion between crystal modification

Table 2.2. I Crystallographic data of crystalline modifications of PVDF

	Unit cell parameters	Space group	Molecular chain	$N^a$
Form I	$a = 8.58 \text{ \AA}$ , $b = 4.91 \text{ \AA}$ , $c$ (f.a) = $2.56 \text{ \AA}$	$Cm2m-C_{2v}^{14}$	Slightly twisted Planar-zigzag	2
Form II	$a = 4.96 \text{ \AA}$ , $b = 9.64 \text{ \AA}$ , $c$ (f.a) = $4.96 \text{ \AA}$ , $\beta = 90^\circ$	$P2_1/c-C_{2h}^5$	TGT $\bar{G}$	2
Form II <sub>p</sub>	Essentially the same as form II	$P2_1cn$ (?)	TGT $\bar{G}$	2
Form III	$a = 4.96 \text{ \AA}$ , $b = 9.58 \text{ \AA}$ , $c$ (f.a) = $9.23 \text{ \AA}$ , $\beta = 92.9^\circ$	$Cc-C_s^4$	TTTGT $\bar{T}\bar{G}$	2

<sup>a</sup> $N$  = number of chains in a unit cell; f.a. = fiber axis.

Crystallographic data of the crystalline structures is described in table 2.2.I.

The  $\beta$  crystalline form consists of the molecular chains crystallized into extended chain crystal and the molecular conformation is all-trans planar zigzag. Orthorhombic unit cell is in the space group  $Cm2m-C_{2v}$  where two chains are packed with  $CF_2$  groups parallel to the  $\beta$  axis. The  $\beta$  form is formed by stretching at room temperature and  $\alpha$  form is formed when the melt is cooled at  $10^\circ C/min$ .<sup>7</sup> Distortion of  $\beta$  phase happens because the fluorine atoms are so large that cannot have regular all-trans conformation.  $\alpha$  phase is in trans-gauche-trans-gauche conformation. Steric Hindrance between the fluorine atoms distorts the conformation. There is large dipole moment between carbon and fluorine atoms so the net dipole moment is perpendicular to the chain axis. Because the unit cell is nonpolar, there are two chains whose direction of dipole moment is opposite to each other. It has lowest

energy molecular conformation.  $\gamma$  has smaller dipole moment than  $\beta$  does and it has trans-trans-trans-gauche-trans-trans-trans-gauche conformation.  $\delta$  has the same conformation to  $\alpha$  but while  $\delta$  has parallel dipole moment,  $\alpha$  has antiparallel orientation. When high electric field above 100Mv/m is applied,  $\alpha$  may be converted to  $\delta$  and higher electric field above 500 MV/m let  $\delta$  phase become  $\beta$ . Polar crystalline  $\alpha'$ ,  $\beta$  and  $\gamma$  phases are capable of permanent and electric field induced macroscopic remnant polarization. However, soon electric field induced dipole orientations in the amorphous phase become random. <sup>1</sup>

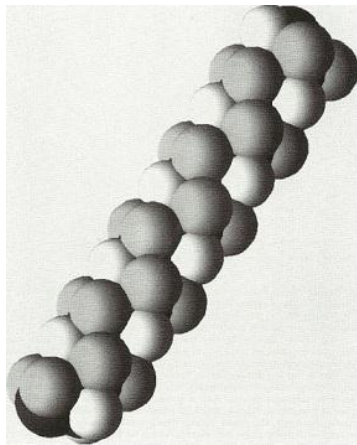


Figure 2.2. 3 PVDF molecule in  $\alpha$  phase

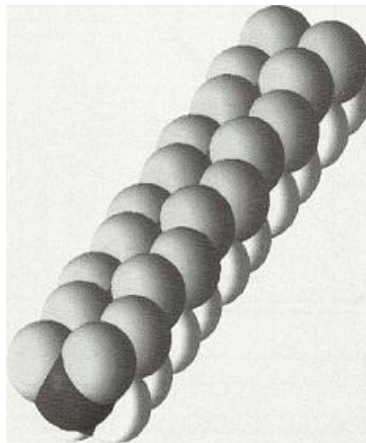


Figure 2.2. 4 PVDF molecule in  $\beta$  phase

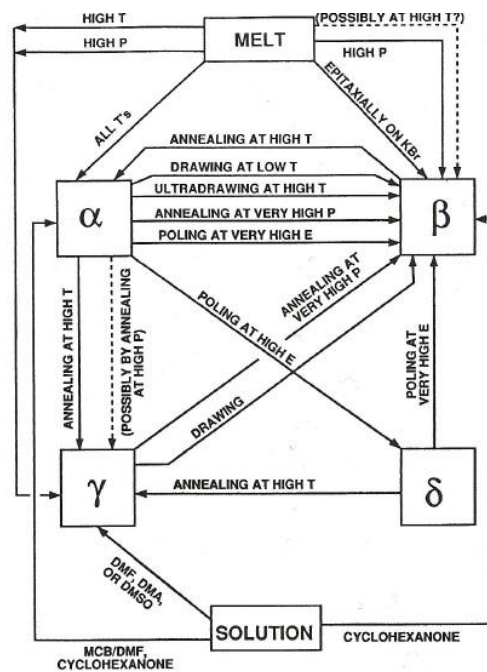


Figure 2.2. 5 Interrelation among four phases of PVDF

## 2.3 Piezoelectricity

Piezoelectric materials have the ability to generate electric current when mechanical stress is applied. The voltage generated is proportion the applied mechanical stress.<sup>8</sup> The first synthetic piezoelectric material was Barium Titanate which exhibits the inverse piezoelectric effect where a voltage applied to the material results in a deformation that can be measured.<sup>9</sup> Some materials such as cane sugar, silk and wood have piezoelectric properties because of their crystal structure.<sup>10</sup> Polypropylene and polystyrene are examples of synthetic polymers which have piezoelectric properties, but the effect is weak and unstable.<sup>11</sup> Broadhurst and Davis claim that there are four criteria needed for polymers to become and remain piezoelectric: the presence of permanent molecular dipoles, the ability to orient and align dipoles, the ability to sustain the dipole moment and the ability to ensure large strain under the mechanical stress. Polyvinylidene fluoride (PVDF) is the only polymer that satisfies all four criteria and demonstrates strong and stable piezoelectric properties. The piezoelectric effect is created when PVDF is stretched; the amorphous region is aligned in a plane and allows the crystalline phase to rotate in an electric field.

<sup>2</sup> The electrical response of piezoelectric materials is a function of stress and the strain and piezoelectric effect can be explained by tensors as in Figure 2.3.1. A net dipole moment exists along the direction 3 when polarization is separation of the positive and negative charges. The piezoelectric effect is the combination of electrical behavior,  $D=\epsilon E$ , and Hooke's Law,  $S=sT$ , where  $D$  defined as volumetric charge density,  $\epsilon$  as the permittivity,  $E$  as electric field

strength,  $S$  as the strain,  $s$  as the compliance and  $T$  as the stress. The piezoelectric coefficient relates the applied electric field to the strain in the same direction. While other materials expand, PVDF compresses under the same applied electric field.

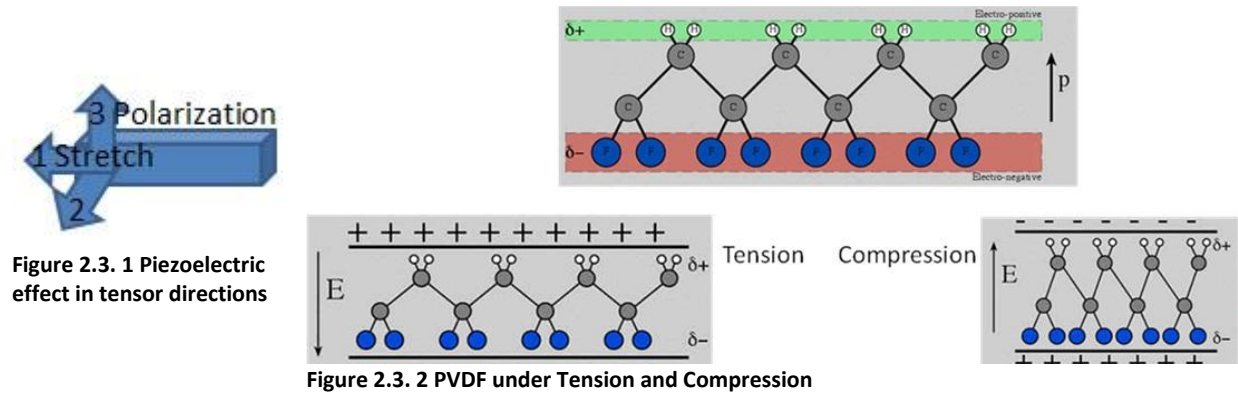


Figure 2.3.2 shows that voltage and current have opposite signs under tensile and compressive stresses. This is because a compressive stress in direction 3 or tensile strength in direction 1 or 2 results in polarization and positive piezoelectric coefficient.<sup>12</sup> Piezoelectric effect is change in the polarization of the material when force is applied; its effect can be recognized by the change in the number of dipole moment of monomer units when local field with stress changes. Reversible changes in crystallinity with the stress might affect piezoelectricity but there is no tangible evidence. One way to improve piezoelectricity is poling process in which polymer is heated and high voltage is applied then the temperature is lowered. During this process macroscopic separation of charge happens. Other way to improve piezoelectric property of PVDF is chemical modification through copolymerization with trifluoroethylene

or tetrafluoroethylene.<sup>6</sup> PVDF is miscible with other polymers which have strong molecular electric moment because of its strong electric dipole in its monomer unit.<sup>1</sup>  $\beta$  phase exhibits the strongest pyro and piezoelectricity. Crystalline structure of PVDF influences the polarity and while  $\alpha$  phase is nonpolar,  $\beta$  phase is polar. When PVDF chains are crystallized in the piezoelectric  $\beta$  phase, all hydrogen atoms are move to one side and fluorine to opposite side. When mechanical stress is applied to the  $\beta$  phase, hydrogen and fluorine atoms shift relative to each other and generate an electric dipole and field.<sup>13</sup> In order to have power generation property, fibers must have  $\beta$  phase PVDF crystals.

#### **2.4 Solvent-non-Solvent System**

Solution form is needed to electrospin the fibers. Usually, solvent is used to dissolve polymer into the solution. There are several solvents available for as shown in table 2.4.I. PVDF and while more options are suitable for lower molecular weight, solvent options get narrower as molecular weight increases. Solvent evaporates faster when the concentration of the solution is low.<sup>14</sup> Also, solvent and its dipole moment have influence on forming different crystalline phases. Table 2.4.II shows the dipole moment of few samples and when its value is lower, more  $\alpha$  crystalline phase tends to form. When the value increases, the amount of  $\beta$  crystalline phases also increases. Non-solvent can be added in the solution when it has benefits during the process. Acetone is latent solvent which requires heat to dissolve PVDF. 100v% acetone can be

used as solvent at high temperature. It impedes the formation of droplets and improves homogeneity. While acetone makes the solution less viscous, it has high volatility. Usually solution with lower viscosity requires the higher limit of spinnable concentration. Higher viscosity of the solution results in thicker fibers. Thus, increase in acetone which makes the solution less viscous reduces the diameter of the fibers. <sup>15</sup>

**Table 2.4 II List of solvents for PVDF**

Active Solvent	Boiling Point (°C)	Flash Point (°C)	Latent Solvent	Boiling Point (°C)	Flash Point (°C)	Latent Solvent	Boiling Point (°C)	Flash Point (°C)
Tetrahydrofuran	65	-17	Acetone	56	-18	Ethyl Acetoacetate	180	84
Methyl Ethyl Ketone	80	-6	Methyl Isobutyl Ketone	118	23	Butyrolactone	204	98
Dimethyl formamide	153	67	Glycol Ethers	118	40	Isophorone	215	96
Dimethyl acetamide	166	70	Glycol Ether Esters	120	30	Triethyl phosphate	215	116
Tetramethyl urea	177	65	N-Butyl Acetate	135	24	Carbitol Acetate	217	110
Dimethyl Sulfoxide	189	35	Cyclohexanone	157	54	Propylene Carbonate	242	132
Trimethyl phosphate	195	107	Diaceton Alcohol	167	61	Glyceryl triacetate	258	146
N-Methyl-2-Pyrrolidone	202	95	Diisobutyl Ketone	169	49	Dimethyl Phtalate	258	149

**Table 2.4 I Dipole moment of solvents**

Solvent	Moment(D)
THF	1.75
MEK	2.76
Acetone	2.91
DMAc	3.72
DMF	3.86
DMSO	3.96

However, since the jet concentration increases rapidly during the process due to the high volatility of acetone, the initial concentration needed is lower than the solution without the acetone.<sup>14</sup> While acetone can lower the spinnable concentration, it can also affect the crystalline phase formation. The solvent evaporation rate is largely responsible for formation of crystalline phase and because acetone is added to change the evaporation it affects the crystalline formation.<sup>16</sup> Also, its low evaporation temperature helps to decrease the amount of  $\alpha$  phase. The solvent evaporation is mainly responsible for the formation of the  $\beta$  phase and  $\beta$  phase preferably formed with low evaporation rate and  $\alpha$  phase with high rate.  $\alpha$  and  $\beta$  phase coexist with intermediate rates. Moreover, acetone also increases the enthalpy of fusion so as percent crystallinity.<sup>14</sup> Costa et al. claims that drawing process is not critical to  $\beta$  phase formation.

## **2.5 Electrospinning**

Electrospinning is a simple method for drawing polymer fibers with diameters at nano or micron scale using high voltage supply.<sup>17</sup> The products vary with temperature, feeding rate, applied voltage, diameter of the needle, distance between the needle tip and the ground and the conductivity of the collector.<sup>18</sup> Fibers surely depend on the viscosity, conductivity and surface tension of the solution resulted from polymer type and its molecular weight, concentration of

the solution and solvent composition and its evaporation rate. Theron et al. observed that usually polymers with low conductivities work well for electrospinning.<sup>19</sup>

Electrospun fibers are semicrystalline and have characteristics of high porosity, small diameter, excellent pore interconnectivity and high surface to volume ratio. Also, electrospun fibers can be uniaxially aligned over long length in centimeter scale.<sup>20</sup> There are several ways to produce nanofibers; chemical vapor deposition (CVD), molecular self-assembly, nanofiber seeding method, electrospray deposition (ESD), and electrospinning.<sup>15</sup> Electrospinning is an economical spinning process simpler than other spinning. While electrospray requires lower concentration, it generates films with small droplets rather than fibers.<sup>21</sup> Products obtained from electrospinning displays higher degree of crystallinity than that from electrospray. Also, drawing during electrospinning helps nanofibers to form in the direction of favorable orientation of the chains.<sup>14</sup> The nano scale fibers spun from electrospinning process is useful to filtration, membrane separation, thermal insulation and manufacture of protective clothing, sensors, conducting devices, wound dressings and scaffolds for tissue engineering.<sup>22</sup>

Fibers spun from PVDF solution may have different crystalline phases depending on the spinning condition. Moreover, those formed phases can be reversible by the external factors such as high pressure and high voltage. Research shows that an inversion of  $\text{CF}_2$  dipoles or reorientation of the crystal lattice happens under electric field. The difference can be distinguished using

X-ray diffraction which shows different intensity.<sup>3</sup> Electrospinning produces piezoelectric  $\beta$  phase PVDF fibers by the mechanical force of drawing. However, when the molecular chains are not highly aligned relative to each other, the fibers will not have piezoelectric property. Fibers are formed by buildup of charge at the surface of the polymer solution droplet to push towards a grounded substrate. During the electrospinning process, at the tip of the syringe needle, the solution forms a droplet called the Taylor cone due to the surface tension and it is affected by the voltage applied. If the voltage creates the force greater enough to overcome the surface tension, Taylor cone becomes thin jet. Thompson et al. concluded that larger diameter of the initial jet results in larger diameter of the fibers. They also found that applied voltage affects the size of the Taylor cone.<sup>23</sup> This jet with whipping instability accelerates as it gets closer to the ground. When the viscosity of the solution controlled by the concentration is adequate, the jet becomes stable. Before jet reaches the ground, the polymer solution is stretched due to the electric field applied and the solvent evaporates. This process results in ultrathin fibers and formed as a randomly oriented pile of nonwoven fibers on the collector.<sup>14</sup>

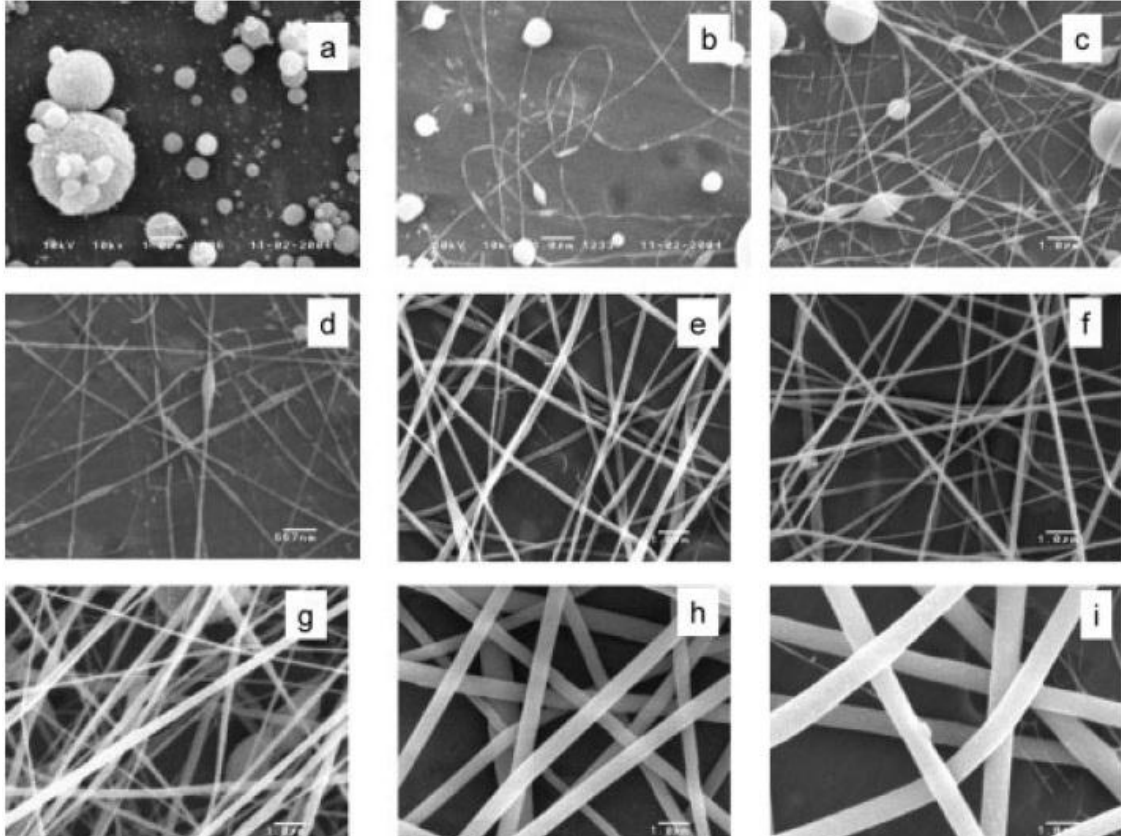


Figure 2.5. 1 Morphology of nanofiber from PVDF solution at different concentration

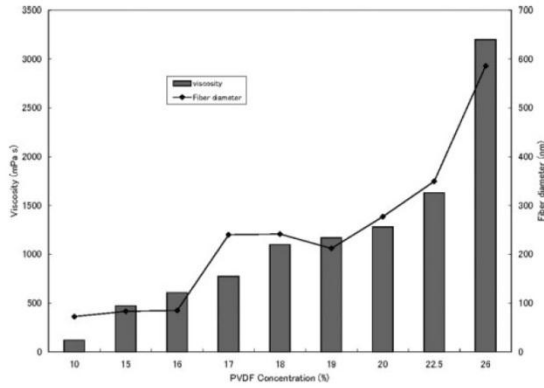


Figure 2.5. 2 Effect of polymer concentration on polymer viscosity and fiber diameter

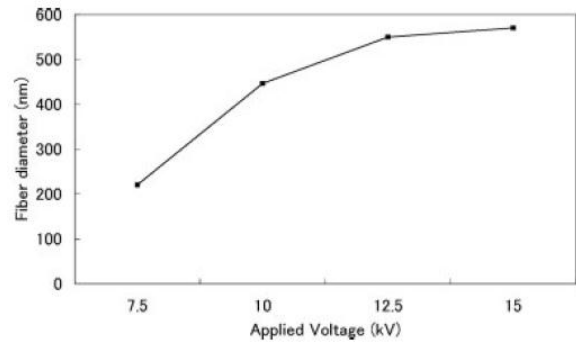


Figure 2.5. 3 Effect of applied voltage on fiber diameter from 26wt% PVDF/DMAc solution

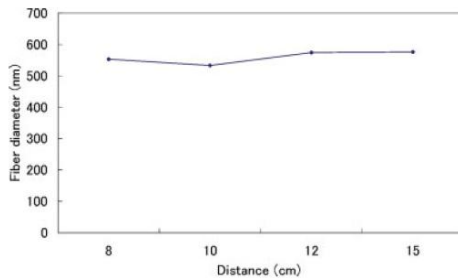


Figure 2.5. 4 Effect of distance on fiber diameter from 26wt% PVDF/DMAc solution

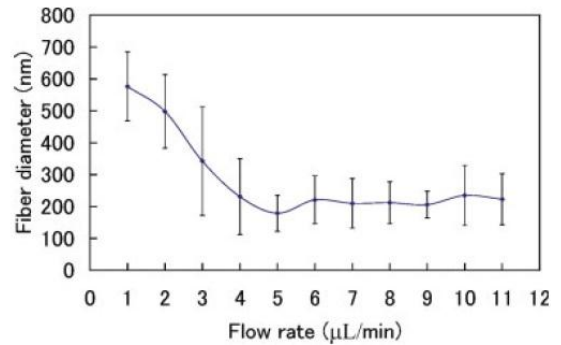


Figure 2.5. 5 Effect of flow rate of the polymer solution on fiber diameter

Formation of the fiber greatly depends on the polymer concentration. Effect of polymer concentration on solution viscosity and fiber diameter is shown in figure 2.5.2. When the concentration is not ideal, the electrospun sheet shows some droplets. At low polymer concentration, mainly beads are formed and as the concentration increases fibers starts forming. The number of beads decreases with increasing concentration. Bead formations are affected by instability of jets, controlled by the combination of concentration, viscosity, surface tension and electric force.<sup>24</sup> The study concludes that the diameter of the fiber increases with the concentration of PVDF. As shown in figure 2.5.3, increasing applied voltage also leads to increase in the fiber diameter because the force which overcomes the surface tension rises. However, figure 2.5.4 gives evidence that there is no significant effect with distance change between the needle tip and the collector. When the distance increases, the electrical field strength, which influences the continuous stretching, decreases, but the time allowed for solvent to evaporate increases. Figure 2.5.5 indicates that the fiber diameter decreases when flow rate increases. However, increasing the feeding rate may also increase the electrical current depending on the polymer solution. If the surface charge density decreases when the flow rate increases, it will result in decrease in the fiber diameter. <sup>19</sup>

## CHAPTER 3

### EXPERIMENTAL APPROACH

#### **3.1 Materials**

Poly(vinylidene fluoride)(PVDF)(Mw ~ 530,000g/mole) in a pellet form was obtained from Sigma-Aldrich(Milwaukee, WI). N,N-Dimethylacetamide from Sigma-Aldrich(Allentown, PA) was used as a solvent and acetone from VWR(Philadelphia, PA) was used as non-solvent.

#### **3.2 Instruments**

The solution was mixed and stored in 20ml vial with a stir bar inside and the hot plates were used during the process of mixing. Parafilm was taped around the lid to prevent solvent evaporation.

5mm plastic syringes and needles with diameter of 1mm were used for solution containment during the electrospinning process. Harvard apparatus syringe pump was used for feeding the solution. Aluminum foil wrapped on the sheet of the copper plate was served as a collector. The voltage was supplied by voltage source.

AR2000 stress-controlled rheometer from TA Instruments (New Castle, DE) with the concentric cylinder geometry with an external fluid circulator for temperature control was used for the rheological analysis.

Leica 440 Scanning Electron Microscope was used to capture the images of the electrospun samples. The samples were sputter-coated with Au beforehand

and SEM was operated at 10kV. The diameter of the fibers measured from the images captured from SEM using ImageJ, a public domain Java image processing program written by Wayne Rasband (Research Services Branch, National Institute of Mental Health, Bethesda, MD).

TA Instruments Q2000 Differential Scanning Calorimetry was used to characterize the glass transition temperature, melting temperature and the entropy of each sample and total crystallinity was calculated based on the data.

Scintag Theta-Thea X-ray Diffractometer helped to determine the percent crystallinity of different phases existing in PVDF as well as the total crystallinity.

### **3.3 Experimental Procedures**

#### **3.3.1 Electrospinning Experiments**

The schematic of the electrospinning setup is in Figure 3.3.1. The syringe contains a charged polymer solution droplet and the solvent evaporates while traveling from the needle tip to the grounded substrate then, dry PVDF fiber is deposited selectively on the grounded aluminum foil. When the charge buildup on the surface of the forming fiber is positive, fluorine which has opposite charge to positive will be at the exterior of the fiber and the hydrogen which has positive charge will be found at the interior. Using the syringe pump which has flow rate adjustability, the feeding rate was varied between 0.01ml/min and 0.06ml/min. The syringe was surrounded by the system which changed

the temperature of the solution while spinning. For each solution, three different temperatures, 25°C, 40°C and 55°C, were used and approximate elapsed time for each run was 10 min. The tip of the needle was connected to the voltage source. The distance from needle tip to the collector was kept between 12 and 15cm. The voltage applied was varied from 15kV to 18kV for better Taylor cone forming. A copper sheet covered with the aluminum foil was used as the grounded collector where the fibers are collected. For each solution, three different temperatures, 25°C, 40°C and 55°C, were used and approximate elapsed time for each run was 10 min.

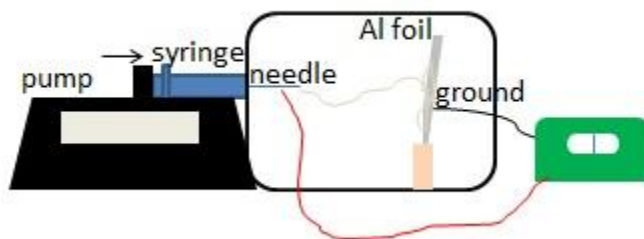


Figure 3.3. 1 Electrospinning setup

### 3.3.2 Rheological Experiments

In order to minimize acetone evaporation whose volatility is 100% and evaporation rate is 7.7, the surrounding of the machine was wrapped with aluminum foil and acetone was put inside to saturate the atmosphere. The surface of the 60mm standard steel parallel plate was lowered to 5°C because rate of evaporation can be lowered when the temperature decreases. After

loading the sample, the gap between two plates was lowered to 1000micron as shown in figure 3.3.2.

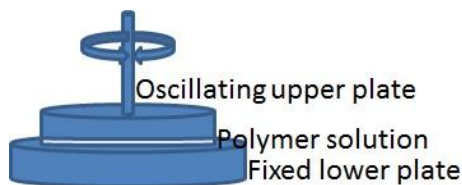


Figure 3.3. 2 Rheometer setup

Strain sweep from 1% to 100% was exercised at 25°C. Several frequencies from 2rad/s to 6rad/s was tried to distinguish clear linear viscoelastic regions of each solution. After that region was identified, %strain at the borderline of the plateau region was selected. The chosen %strain was used for temperature ramp in which temperature was decreased by 1°C from 55°C to 25°C and at each temperature, frequency changed from 1rad/s to 100rad/s. Frequency sweep tests are used to evaluate the viscous and elastic components of the solution under oscillation stress. Then, steady state flow produced viscosity and shear stress depending on shear rate from 0.01/s to 100/s. Lastly, viscosity vs time was measured although there was no change since the duration of the experiment was not enough time-dependent-gelation to be happened.

### 3.3.3 SEM Image Analysis

In order to characterize the morphologies of the electrospun PVDF fibers, scanning electron microscopy (SEMs) captured images at several

magnifications. From the images, 50 to 100 measurements of the fiber diameter were obtained using ImageJ. The average diameters for each solution are included in section 4.3.

#### **3.3.4 % Crystallinity from DSC**

The heating rate was set to 5C/min from -45°C to 190°C and the sample was cooled to -45°C and re heated to 190°C at the same rate. Heat of fusion was determined by peak area in the curves and it was used to calculate the total crystallinity of the sample by comparing the heat of the fusion of 100% crystalline PVDF which is 104.7J/g.

#### **3.3.5 % Crystallinity from XRD**

SCINTAG theta-theta diffractometer was used for Wide angle X-ray diffraction(WXAD) with a standard Cu at 45kV and 40mA. The range of the diffraction angle( $2\theta$ ) during the scan was from 2 to 35 with a scan rate of 5 deg/min.

#### **3.3.6 Statistical Analysis**

JMP was used to see the combined effect of the three variables; concentration, spinning temperature and volume percent of acetone in solvent. The fit model was created based on the data from the experiments. Surface response model predicted the % $\beta$  Crystallinity which also includes the combination that was not experimented.

## CHAPTER 4

### RESULTS AND DISCUSSION

#### **4.1 Electrospinning**

PVDF fibers were spun using electrospinning process by investigating effect of PVDF concentration, spinning temperature and solvent composition on crystallinity and each crystalline phase. The effect of all three variables is interconnected because the solvent evaporation rate increases with lower concentration of polymer in solution and at higher spinning temperature. Since acetone used in solvent system is very volatile, the influence of polymer concentration and spinning temperature is critical. The interaction between good solvent, DMAc, and poor solvent, acetone, in solvent system cannot be negligible as well. When the amount of acetone is kept the same in the solution, if the concentration of polymer in the solution increases, the evaporation rate decreases. However, at the same time, if the spinning temperature during the electrospinning increases, the evaporation rate increases. The evaporation rate also changes with the change in the volume percent of acetone in the solvent. Thus, these factors have complex relationship because the effect of each parameter differs for other two factors. In other words, the effect of concentration to slow the evaporation of the solvent may influence more at lower spinning temperature than higher.

It is best if the solvent can evaporate all during the whipping motion from needle tip to collector. If the solvent reaches collector, the residual solvent can

both melt the fiber and change the crystallinity during the evaporation. With low concentration of PVDF polymer (< 12 %) in the solution primarily beads and few fibers are produced for any solvent composition or temperature.<sup>20</sup> As the PVDF concentration the number beads decreases and more uniform fibers are formed. In the solvent system, the ratio between DMAc and acetone varied from 1:1(50v%acetone) to 1:6(86v%acetone). Addition of a non-solvent in electrospinning is helpful to increase the relative polymer concentration in the good solvent while maintaining low viscosity.<sup>15</sup> Thus, it is possible to electrospun solution containing lower polymer concentration in to fibers. Increasing the acetone fraction in the solvent decreased the prevalence of beads in the fiber and also resulted in finer fiber diameters.

Samples were spun at 25°C, 40°C and 55°C. Temperature higher than 55°C was not investigated since the boiling point of the acetone is 56°C. When the temperature increases, few changes in solution happens including decreased viscosity, increased solvent evaporation rate and possible transition between solution and gel phase. During the experiment, some electrospun conditions, applied voltage, distance between needle tip to collector and feeding rate, varied in small range to create the spinnable conditions. Because the spinnability is more affected by the PVDF concentration and the solvent composition, those variation is negligible and the literature review in chapter 2 also supports this. However, those parameters were tried to be kept closer to create the condition for the better comparison. Thus, the parameters chosen are not the best condition to produce fibers.

Electrospinning parameters are important for producing fibers to maximize  $\beta$  crystalline phases responsible for piezoelectric properties. But also it is important to improve the morphology of the fibers to small diameter and uniformity needed for incorporating into applications. Even with high %  $\beta$  crystallinity if it cannot be used in devices, there is no use. Thus, electrospinning condition is required to consider both criteria.

## 4.2 Rheological Analysis

Molecules in polymer solution keep adopting many conformations rather than being stationary and these different conformations can alter the flow properties of polymer solutions. Temporary entanglements and intermolecular physical polymeric networks might be formed in solution and the oscillatory shear curves depend on them.<sup>25</sup> Gel formation of the solution is a function of the polymer concentration and the temperature. Four samples which have relatively high viscosity are investigated. Since parallel plates are used, solutions with low viscosity will not be measured properly. Even though there is other geometry available for low viscosity solution, parallel plates are selected for two reasons. One is that there is a solvent trap available for that geometry and second is that the state of the solution after the experiment is easily observed. The gelation happens within a few weeks for most samples and it happens faster for more viscous samples. The samples chosen go through gelation within few days without external influences. The solution with 18wt%PVDF mixed with the solvent of 70v%acetone and 30v%DMAc (18D3A7), 16wt%PVDF mixed with 83v%acetone and 27v%DMAc (16D1A5), both 16 and 18wt%PVDF mixed with the solvent of 86v%acetone and 14v%DMAc are chosen (16D1A6 and 18D1A6). The solution with the same PVDF concentration with two different acetone volume percent are chosen to see the effect of acetone on viscosity. Also, two different PVDF concentrations with the same solvent composition are chosen to see the influence of concentration with acetone on viscosity. Acetone adds complexity to the

rheology experiment as discussed in section 4.1. The volatility of acetone reacts sensitively to both concentration and temperature and its evaporation rate changed. Although solvent trap system has been used, the high evaporation rate of acetone creates uncertainty in remaining amount of acetone in the solution and its change over the time. Thus, acetone might be responsible for some of the abnormal results.

Figure 4.2.1 shows the results under oscillation mode and strain ranges from 1 to 100% at 25°C. The plots used to determine the linear viscoelastic region for each sample and a strain rate at the border of plateau region was chosen for further studies on temperature and frequency dependency. 4rad/s is used for the solution with 16D1A5. 3 rad/s is used for the solution with 16D1A6. 8rad/s is used for the solution with 18D3A7 and 3rad/s for the solution with 18D1A6. All the curves remain steady before the fall and each sample has different plateau region for storage modulus. The level of storage modulus for each sample is different. For 16wt%PVDF samples, the value of the viscoelastic region decreases with increase in acetone while for 18wt%PVDF the opposite trend is observed. With the same solvent composition, the  $G'$  value increases with the concentration. However, it is strange that the level for the 16D1A6 is much lower than that for other samples. This might be related to polymer relaxation. The storage modulus curve depending on strain starts decreasing at certain

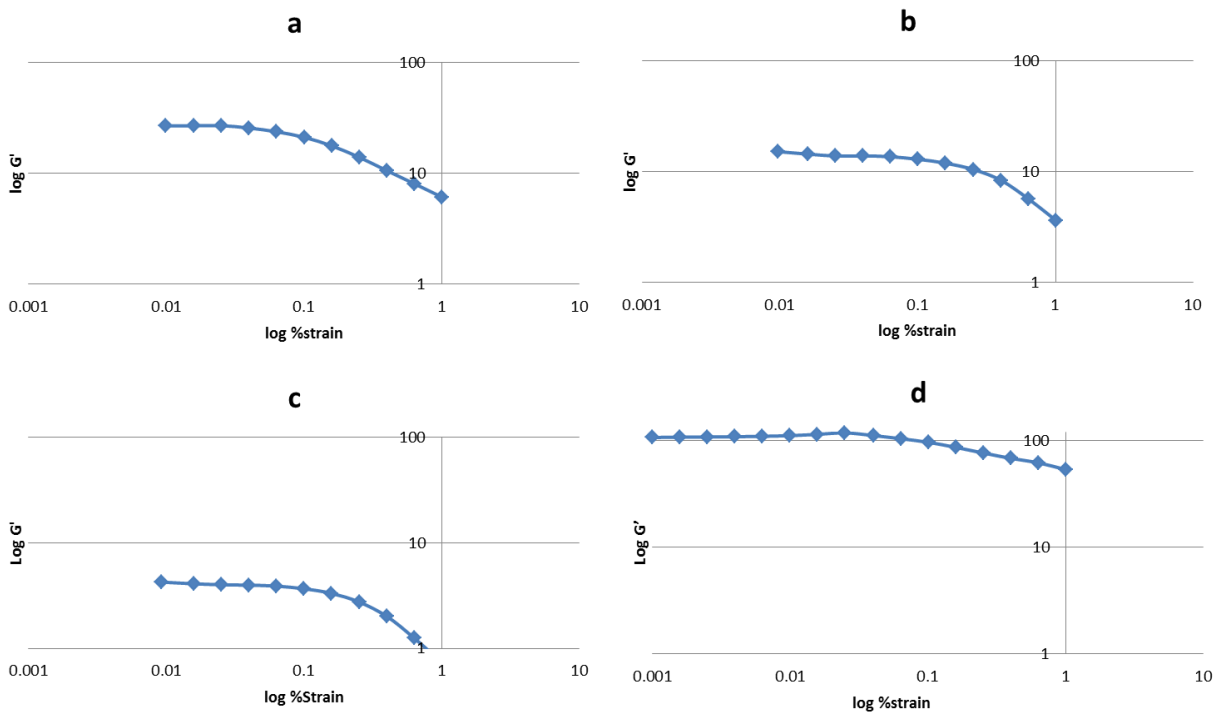


**Figure 4.2. 1 Storage modulus of a) 16wt%PVDF+solvent [83v%Acetone+17v%DMAc]  
 b) 18wt%PVDF+solvent [70v%Acetone+30v%DMAc]  
 c) 16wt%PVDF+solvent [86%Acetone+14%DMAc]  
 d) 18wt%PVDF+solvent [86%Acetone+14%DMAc] depending on %strain**

point which differs for each solution. That means that the strain induced disentanglement of the molecules occurs because the storage modulus response indicates the entanglement density. The maximum strain for the solution with 16D1A5 is about 2.5%. That for the solution with 16D1A6 slightly increases to 5%. That for the solution with 18D1A7 is 2%. Finally, that for the solution with 18D1A6 is 2%. Again, critical strain responds differently, increasing with increase in acetone for 16wt%PVDF but decreasing with increase in acetone content for 18wt%PVDF. With the same solvent composition, the critical strain decreases with increase in PVDF concentration. All the results support that three variables have a complicated combined effect on the solution rheology.

Simultaneous frequency and temperature sweeps are used to see the dependence of viscosity on the temperature. For all the samples, viscosity decreases with increase in frequency and this supports shear thinning behavior of the solution. Figure 4.2.2 is a plot of viscosity depending on temperature at 10rad/s. Normally, viscosity should decrease with the increase in temperature and 18D1A6 solution exhibits that behavior. However, it shows low viscosity and no temperature dependence of viscosity for the solutions made with low volume percent of acetone in solvent. This might be resulted from the fact that they have relatively low concentration over good solvent than 18D1A6. As parallel plate cannot detect change in low viscosity, it is possible that the no dependence is resulted from that. Moreover, theoretically, when more acetone is added to the solvent, acetone makes the solution less viscous compared to using only good solvent. For 16wt% solutions, the viscosity

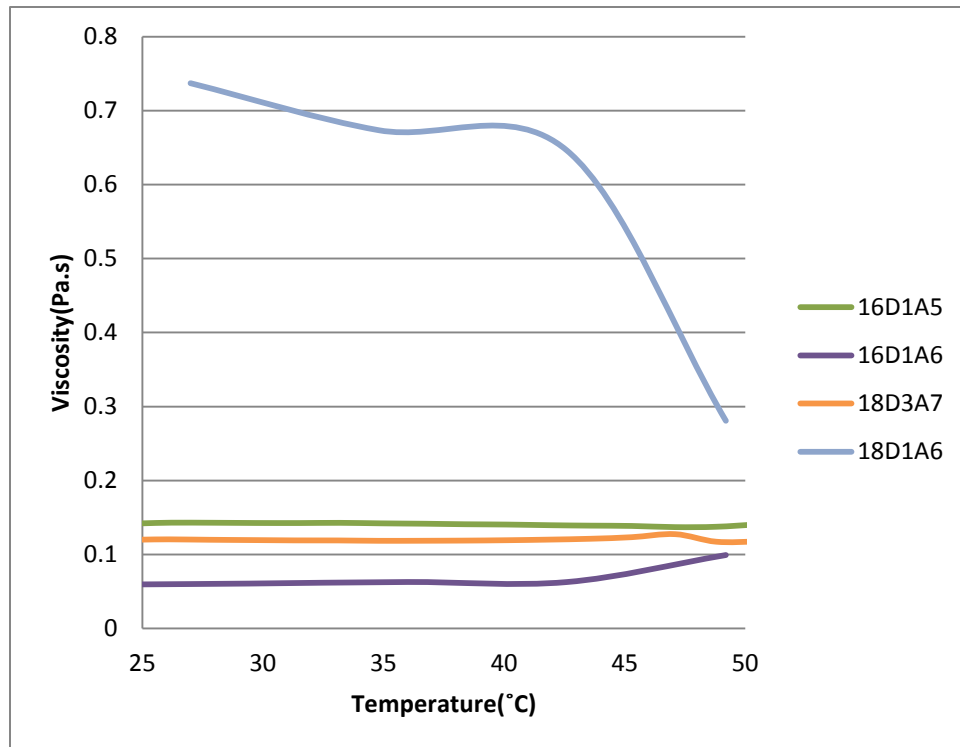


Figure 4.2. 2 Dependence of viscosity on temperature at 10rad/s

decreases when more acetone is added; in the plot 16D1A6 has lower viscosity than 16D1A5. However, it shows that the viscosity of 18D1A6 solution is a lot higher than that of 18D3A7. Even though adding acetone should lower viscosity of the solution and that is the one of the advantage using acetone during the electrospinning, the result does not prove that for 18wt%. This result may state that if the polymer concentration is too high, the effort of acetone lowering the viscosity is not successful. In morphological view of fibers spun from these solutions, when viscosity increases, fiber diameter should increase. Comparing 16D1A6 to 18D1A6 which possess high viscosity, 18D1A6 has slightly larger average fiber diameter. The value of fiber diameter is from spinning temperature of 55°C because 18D1A6 solution is not spinnable at lower temperature as shown in table 4.2.I. The data proves that the solution with higher viscosity result in large fiber diameter. When the fiber diameter is compared between 16D1A5 and 16D1A6, at 40°C, 16D1A6 has thinner fiber in average. In the plot, 16D1A6 solution has the lowest viscosity. Thus, it should produce lowest fiber diameter but it does not. This shows that acetone not only changes the viscosity of the solution but also changes the evaporation rate during the electrospinning. When the acetone evaporates too fast, the solution becomes viscous during the process and produces thicker fibers. In this case though, 16D1A6 has more acetone than 16D1A5. Even though for acetone itself, its evaporation rate will not be changed with the its amount, when it presents in the solution, the polymer can slow the evaporation rate. Thus, this may show that that is only effective till certain amount of

acetone and for 16D1A6 the acetone exceeds this limit and evaporates faster than the one in 16D1A5. For 16D1A6, the evaporation rate has more influence over the viscosity.

**Table 4.2. I Fiber diameters in  $\mu\text{m}$**

	16D1A5	16D1A6	18D1A6
25°C	0.72		
40°C	0.94	1.35	
55°C	0.97	0.93	1.28

Figure 4.2.3 shows the change of storage modulus which represents the entanglement density over the temperature. Storage modulus is higher for high frequency because it causes more residual to structure. However, its dependence on temperature is unnoticeable except for the solution with 18D1A6. It also has very high storage modulus compared to other samples. The change might be resulted from the longer relaxation time and measuring data during relaxing. The sudden change of the storage modulus also can be explained by change of molecular entanglement with temperature. This result showing high entanglement could be the reason that the solution is not spinnable at lower temperature. As shown in figure 4.3.4, there is no difference in the view of morphology while there is difference in entanglement density between 16D1A6 and 18D1A6. Figure 4.3.7 shows that 16D1A5 has thicker fiber diameter and more curvature compared to 16D1A6 and figure 4.2.2 proves that 16D1A5 has more entanglements in the solution.

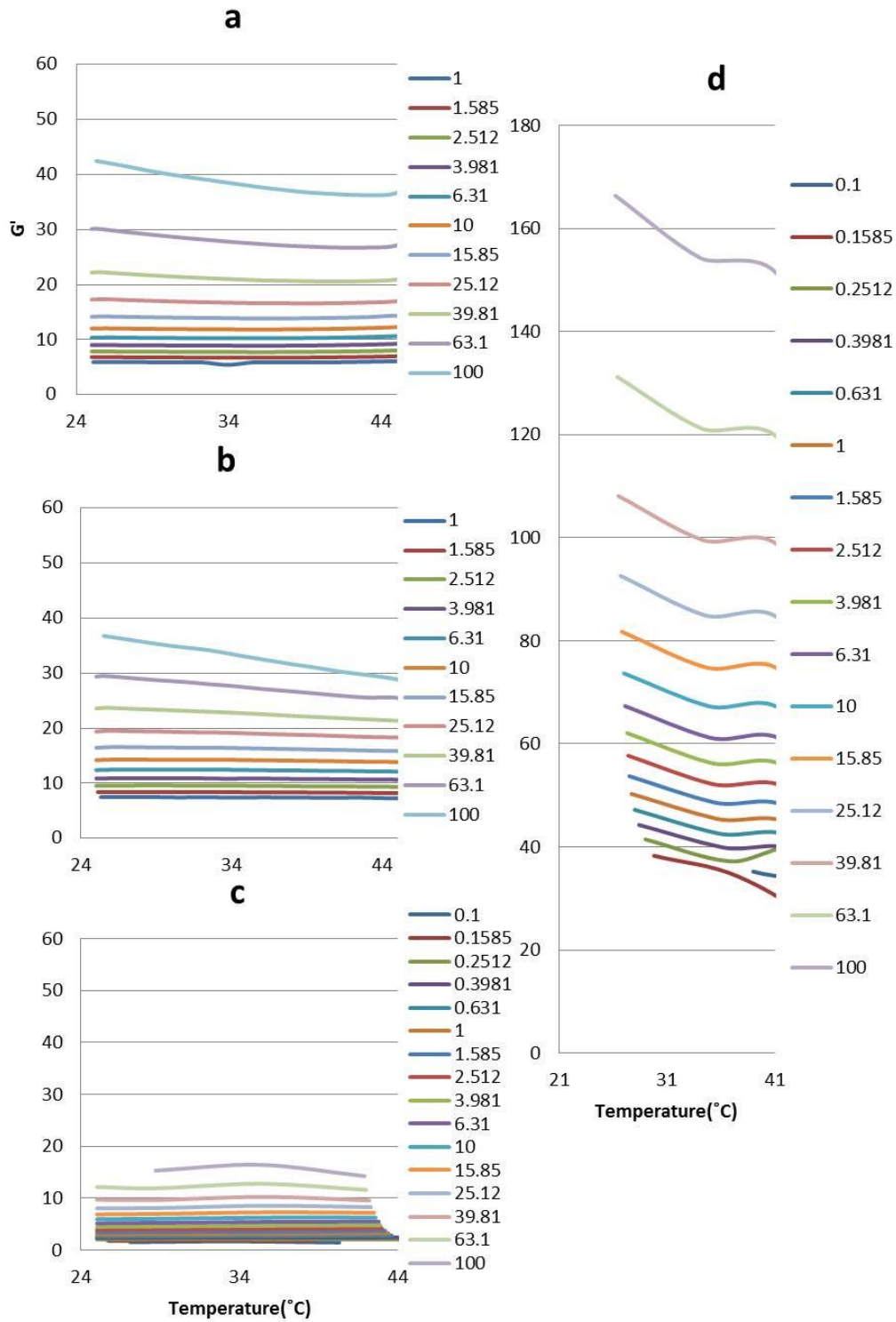


Figure 4.2. 3 Storage modulus of a) 18wt%PVDF+solvent [70v%Acetone+30v%DMAc]  
 b) 16wt%PVDF+solvent [83v%Acetone+17v%DMAc]  
 c) 16wt%PVDF+solvent [86v%Acetone+14v%DMAc]  
 d) 18wt%PVDF+solvent [86v%Acetone+14v%DMAc]  
 at different frequency depending on temperature

The gelation point can be found either the crossover point of the storage modulus and the loss modulus or the inflection point of the Tan delta graph as shown in figure 4.2.4.a and b. The numbers on the sides indicate different temperature. The sample used is the solution with 18D1A6. Both plots suggest that the gelation happens at very low frequency. However, it is abnormal that gelation happens at lower frequency at lower temperature than higher temperature. High frequency results in low average relaxation since they are inversely proportional. Figure 4.2.5.a shows that the behavior of viscosity and the shear stress depending on shear rate. It confirms shear thinning behavior as the viscosity decreases when the shear rate increases, it approaches zero shear viscosity. It also shows that the shear stress is proportional to the shear rate and shear stress increases with increasing shear rate. When gel forms shear stress tends to decrease because internal force resists the deformation. However, gelation is not observed and this means that the gelation takes longer than the electrospinning time scale. The gelation of most viscous solution takes at least few hours at room temperature; gelation happens faster when the viscosity is higher. Figure 4.2.5.b is a behavior of viscosity and storage modulus in 15min at 8rad/s and 25°C. 25°C is chosen because gelation happens faster at lower temperature and it is the lowest electrospinning temperature. There is a slight change of the viscosity after 800s but viscosity lineally increases with time. However, in overall, it shows the little change with the time but it might due to the evaporation of acetone. It is difficult to overcome the volatility of acetone and acetone is evaporating

during exposure of the solution to the air changes the sample contents. Yet, even with the complication with acetone evaporation rate and limited number of samples, the rheology study, important factor in spinning behavior, has some findings. Temperature and frequency dependency of the viscosity and chain entanglement behavior varies with the solution composition and their relations to fiber morphology by SEM images in the next section.

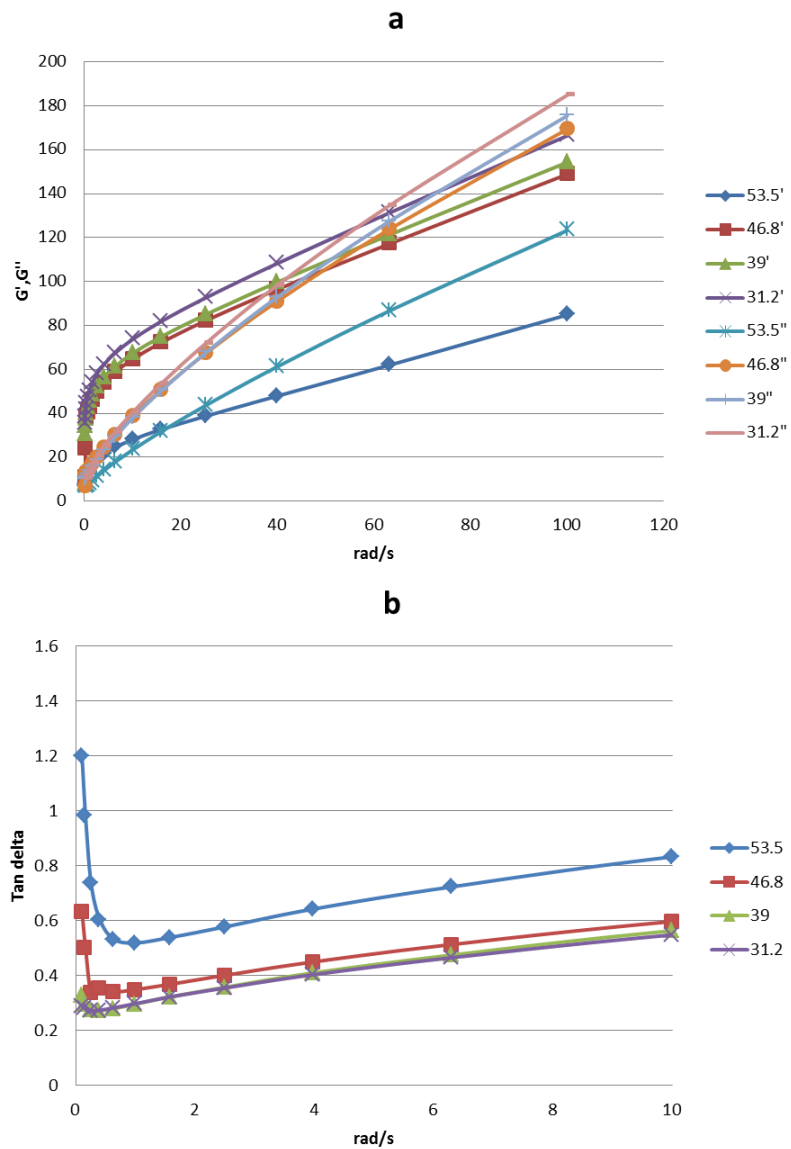
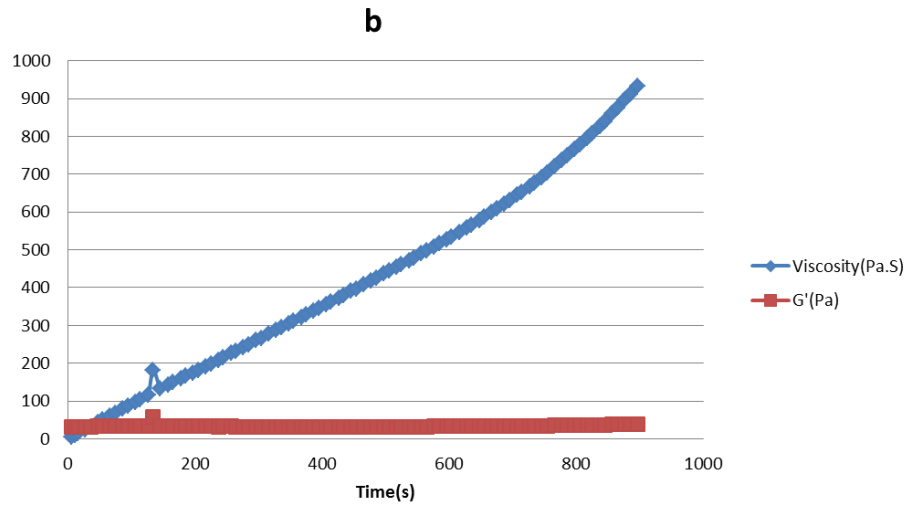
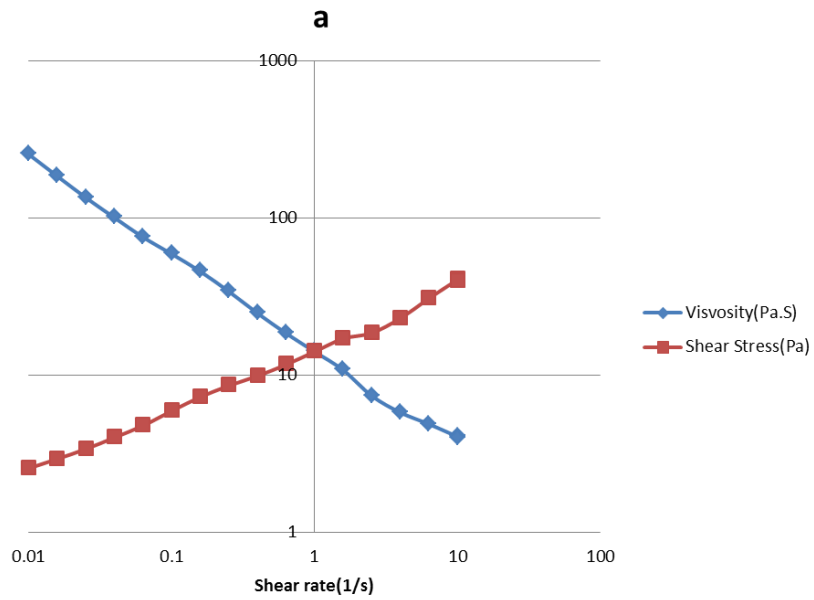


Figure 4.2. 4 For 18wt%PVDF+solvent [86%Acetone+14%DMAc],  
 a) Frequency dependent elastic( $G'$ ) and loss( $G''$ ) moduli and b) Loss tangent( $\text{Tan}\delta$ ) at different frequency  
 c) Flow curves of viscosity and shear stress with the shear rate d) Elastic modulus( $G'$ ) and viscosity as a function of time



**Figure 4.2. 5 For 18wt%PVDF+solvent [86%Acetone+14%DMAc],  
 a) Flow curves of viscosity and shear stress with the shear rate b) Elastic modulus(G')  
 and viscosity as a function of time**

### 4.3 Fiber Morphology

In order to form fibers through electrospinning process, the molecular weight of the polymer and its concentration and solvent have to work together. Even though there are many solvents available to dissolve PVDF into solution, the selection becomes narrower as the molecular weight of PVDF increases. When using PVDF of molecular weight of 53,000g/mole and investigating the concentration between 12wt% and 18wt%, if the volume percent of acetone solvent is less than 50%, fibers are hard to form. The solution with 12wt%PVDF mixed with the solvent of 50v%acetone and 50v% is not capable of producing the fibers while higher concentration with the same solvent system is. The reason for that is lower concentration fails to impede evaporation of solvent. Thus, the acetone which has higher volatility evaporates before forming Taylor cone while it needs to be evaporated during the whipping motion. Some research shows that ability to spin the fibers at the same condition or even with lower volume percent of acetone but the molecular weight is used. The few combinations of acetone and concentration has been chosen first and later the solutions with other combination are investigated as needed to determine the trend of crystallinity depending on the concentration and the acetone ratio. Thus, not all the combination has been spun into fibers although any combination beyond 12wt%PVDF mixed with the solvent of 50v%acetone and 50v% is spinnable. The combinations investigated are noted in Table 4.3.I.

**Table 4.3. I conditions of electrospinning PVDF fibers**

DMAC Conc.	1:Acet.	1 (50v%)	1.5 (60v%)	2.3 (70v%)	4 (80v%)	5 (83v%)	6 (86v%)
12wt% PVDF	25°C	12-20cm		14cm	14cm	14cm	
		13-15kV		15kV	15kV	15kV	
		0.01- 0.05ml/min		0.05ml/min	0.05ml/min	0.05ml/min	
	40°C	12-20cm		14cm	14cm	14cm	
		13-15kV		15kV	15kV	15kV	
		0.01- 0.05ml/min		0.05ml/min	0.05ml/min	0.05ml/min	
	55°C	12-20cm		14cm	14cm	14cm	
		13-15kV		15kV	15kV	15kV	
		0.01- 0.05ml/min		0.05ml/min	0.05ml/min	0.05ml/min	
14wt% PVDF	25°C	14cm			14cm	14cm	14cm
		18kV			15kV	15kV	15kV
		0.05ml/min			0.05ml/min	0.05ml/min	0.05ml/min
	40°C	14cm			14cm	14cm	14cm
		15kV			15kV	15kV	15kV
		0.05ml/min			0.05ml/min	0.05ml/min	0.05ml/min
	55°C	14cm			14cm	14cm	14cm
		15kV			15kV	15kV	15kV
		0.05ml/min			0.05ml/min	0.05ml/min	0.05ml/min
16wt% PVDF	25°C		14cm			14cm	
			18kV			15kV	
			0.05ml/min			0.05ml/min	
	40°C		14cm			14cm	14cm
			18kV			15kV	18kV
			0.05ml/min			0.05ml/min	0.01ml/min
	55°C		14cm			14cm	14cm
			18kV			15kV	18kV
			0.05ml/min			0.05ml/min	0.01ml/min
18wt% PVDF	25°C	14cm		14cm	14cm		
		15kV		15kV	18kV		
		0.05ml/min		0.05ml/min	0.05ml/min		
	40°C	14cm		14cm	14cm		
		15kV		18kV	18kV		
		0.05ml/min		0.05ml/min	0.05ml/min		
	55°C	14cm		14cm	14cm		
		15kV		18kV	18kV		
		0.05ml/min		0.05ml/min	0.05ml/min		

Fiber Morphology varies with the concentration, the spinning temperature and the amount of acetone in the solvent system and their combination. Figure 4.3.1 shows the fibers spun from the solution in which equal volume percent of DMAc and acetone is used as a solvent. When the solvent consist of 50v%acetone and 50v%DMAc, fibers spun with 14wt%PVDF contains more uniform thickness than 18wt%PVDF. However, the solvent that did not evaporate during the process is spotted in several spots along with the fibers spun with 14wt%PVDF solution. The wet fibers resulted from high quantity of solvent present in the solution or its low evaporation rate. Crystallinity of this wet fiber due to remaining solvent can be changed because when residual solvent evaporates fibers can be crystallized. Moreover, the solvent can melt the fiber because it is capable of dissolve PVDF. This can be prevented by either decreasing the concentration which can slow the evaporation or increasing the spinning temperature which encourages solvent evaporation. Addition of more volatile solvent which have high evaporation rate also helps the situation. The evaporation rate of DMAc is low and since the volume percent of acetone is not high, the solvent cannot evaporate rapidly. Thus, when the spinning temperature increases, it helps the solvent to evaporate faster and decrease the amount of solvent reaches collector. For 18wt%PVDF, the range of the fiber thickness is wide even though there are fewer beads. Wide range of fiber thickness is resulted from the competition between the concentration which holds the evaporation and the temperature which promotes the evaporation. Another explanation would be first acetone which

makes the solution less viscous was presented and spun finer fibers. However, during the process, the acetone might have evaporated especially when the temperature is close to the boiling point of acetone. This early evaporation makes the solution viscous and result in thicker fibers. These thicker fibers create large curvatures. When the volume percent of acetone in solvent increases to 80v% shown in figure 4.3.2, comparing to fibers spun from 12wt%PVDF solution, those from 14wt%PVDF solution have many curly structures but they get straighter when the spinning temperature rises. Fibers spun from 12wt%PVDF solution show few beads while the number of beads decreases when the concentrations increases to 14wt%. In the figure, fibers in c, d and e exhibit both  $\alpha$  high crystallinity and  $\beta$  crystallinity. Although d and e have some curly fibers, thickness of fibers seems uniform and the curliness can be stretched into straight fiber during the after treatment when used in application. Also since straighter fibers spun at high temperature do not have high crystallinity, it can be argued that this kind of curliness of the fiber is not related to crystallinity. Figure 4.3.3 shows the fibers spun from the solution with solvent of 83v%acetone and 17v%DMAc. Some orientation can be seen for fibers spun from 12wt%PVDF solution at higher temperature. This solvent composition does not produce good fibers when spun from 14wt%PVDF solutions since some beads start to appear and large blobs at high spinning

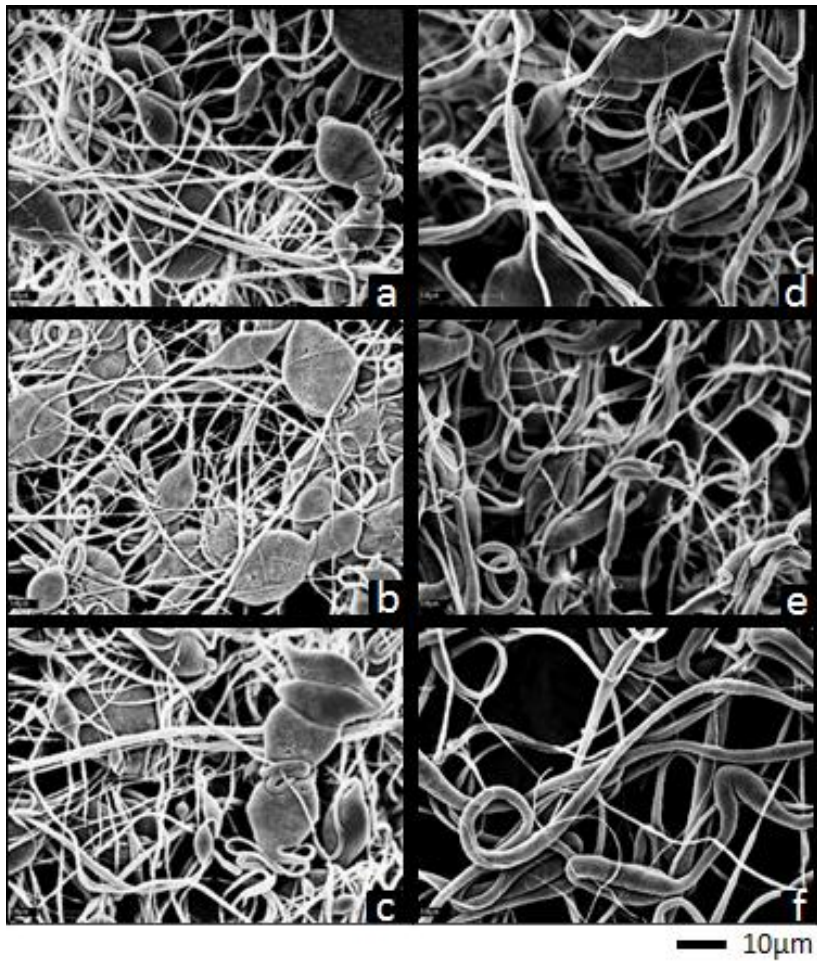


Figure 4.3. 1 SEM images of electrospun fibers from the solution with the solvent of 50v% acetone and 50v% DMAc and 14wt%PVDF spun at (a) 25°C (b) 40°C (c) 55°C and 18wt%PVDF spun at (d) 25°C (ef) 40°C (f) 55°C with the condition of distance at 14cm, voltage at 15kV and flow rate of 0.05ml/min

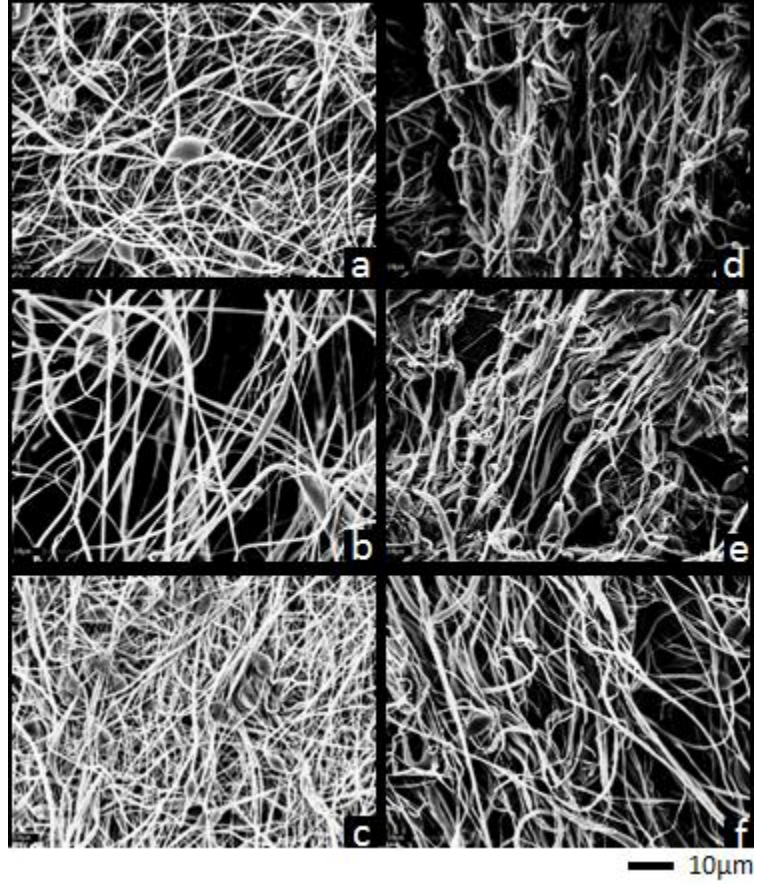


Figure 4.3. 2 SEM images of electrospun fibers from the solution with the solvent of 80v% acetone and 20v% DMAc and 12wt%PVDF spun at (a) 25°C (b) 40°C (c) 55°C and 14wt%PVDF spun at (d) 25°C (e) 40°C (f) 55°C with the condition of distance at 14cm, voltage at 15kV and flow rate of 0.05ml/min

temperature. The images clearly show that increase in fiber diameter at high concentration. However, as increasing temperature should make the solution less viscous and although rheology study above show that low viscosity of the solution with 16wt%PVDF with 83v%acetone in solvent, fibers spun at 55°C has thick fiber diameter. Also, at this concentration it shows in increase in fiber diameter as the spinning temperature increases. Here, high temperature increases evaporation rate too fast, the solution becomes viscous resulting in thicker fibers. The fibers in a and c show high total and  $\beta$  crystallinity. It cannot be explained using only SEM images why fibers from 40°C does not when its morphology is similar to c and better than a. Again, this shows no direct correlation between the fiber morphology and the crystallinity of the fiber. SEM images of Fibers in figure 4.3.4 spun under different spinning condition. Thus, direct comparison between different concentrations cannot be made but overall fibers seem better without any bead than other solvent composition. From the rheology study above, unspinnability of the solution of 18wt%PVDF with 86v%acetone at lower temperature due to high entanglement density. Although, it does not show that for 16wt%PVDF, it is also not spinnable near room temperature. Even though rheology study shows difference in viscosity between those two concentrations, fiber morphology looks similar. This may be due to the fact that acetone may have limitation to lower the viscosity for 18wt%, it can still facilitate the electrospinning process to produce fibers with small diameter. Fibers in b and d exhibit high total and  $\beta$  crsyallinity. Among fibers which shows maximum % $\beta$  crystallinity, those have the best morphology

overall. However, other fibers could have more potential to increase % $\beta$  crystallinity by making better fiber morphology.

From figure 4.3.5 shows the same fibers already discussed above but added to see the effect of adding acetone in solvent on fiber morphology when the concentration kept the same. Figure 4.3.5 shows fibers spun from PVDF solution whose concentration is kept 12wt%PVDF. For the fibers spun from the solution with 12wt%PVDF, higher spinning temperature is not benefit for any solvent composition. However, increasing acetone contents helps to lower the number of beads and produces more uniform and thinner fibers. As stated before fibers spun from 14wt%PVDF solution contains few spots of not evaporated solvent as shown in figure 4.3.6 but increasing the volume percent of acetone in solvent gets rid of remaining solvent on the collector. Fibers in d, e, j and l all have high total and  $\beta$  crystallinity but their morphologies are different although those exhibit better morphologies than others in the figure. Strangely, 83v%acetone does not have benefit in fiber morphology. It might be explained by the effect of relatively high concentration to slow the evaporation rate is too strong. Adding more acetone exceeds 16wt% limit as discussed earlier to hold the evaporation and start helping forming better fibers by evaporating adequately.

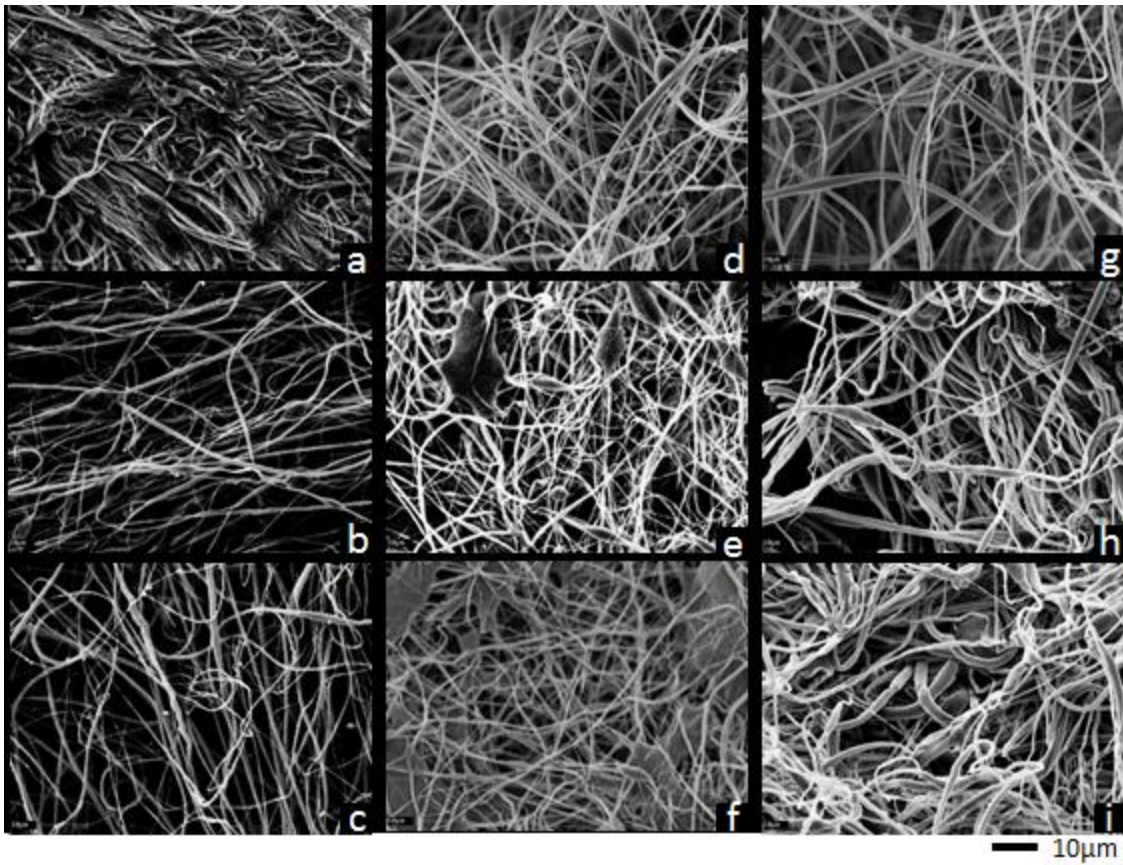


Figure 4.3. 3 SEM images of electrospun fibers from the solution with the solvent of 83v% acetone and 17v% DMAc and 12wt%PVDF spun at (a) 25°C (b) 40°C (c) 55°C and 14wt%PVDF spun at (d) 25°C (e) 40°C (f) 55°C and 16wt%PVDF spun at (g) 25°C (h) 40°C (i) 55°C with the condition of distance at 14cm, voltage at 15kV and flow rate of 0.05ml/min

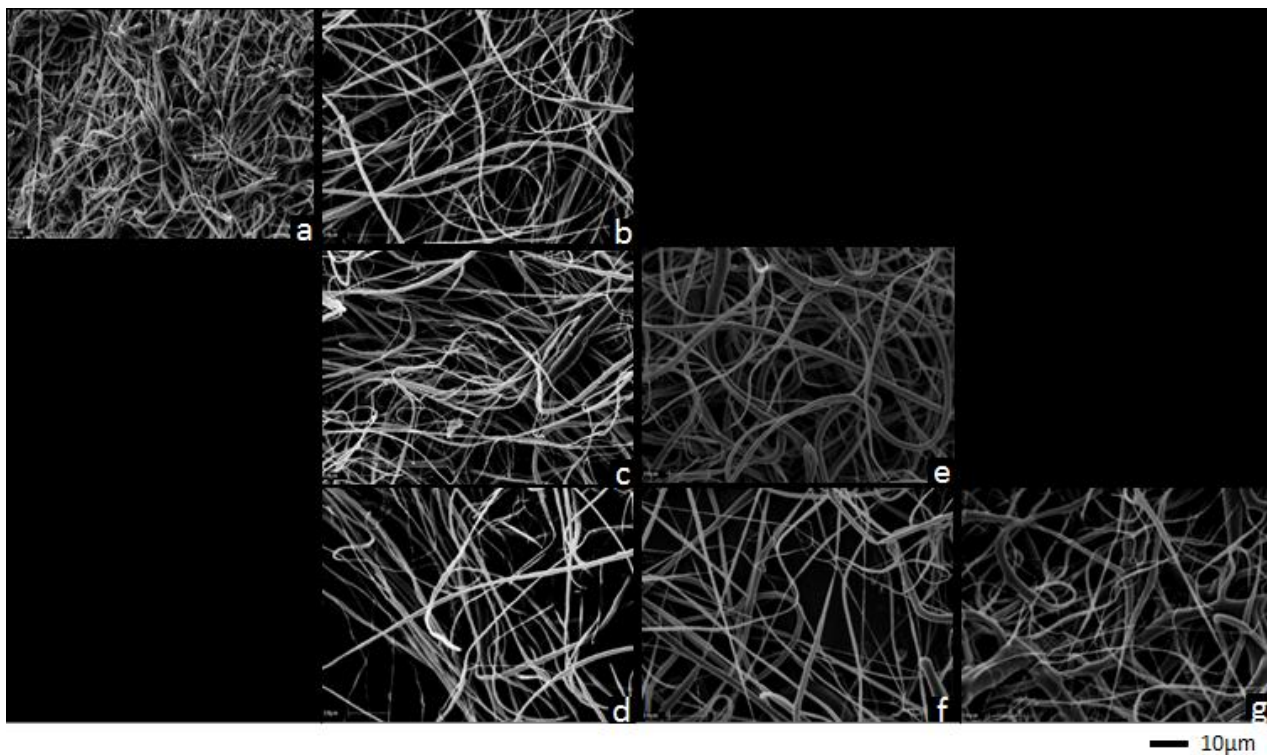


Figure 4.3. 4 SEM images of electrospun fibers from the solution with the solvent of 86v% acetone and 14v% DMAc and 12wt%PVDF spun at (a) 25°C with the condition of distance at 12cm, voltage at 15kV and flow rate of 0.01ml/min 14wt%PVDF spun at (b) 25°C (c) 40°C (d) 55°C with the condition of distance at 14cm, voltage at 15kV and flow rate of 0.05ml/min 16wt%PVDF spun at (e) 40°C (f) 55°C with the condition of distance at 14cm, voltage at 18kV and flow rate of 0.01ml/min 18wt%PVDF spun at (g) 55°C with the condition of distance at 13cm, voltage at 20kV and flow rate of 0.01ml/min

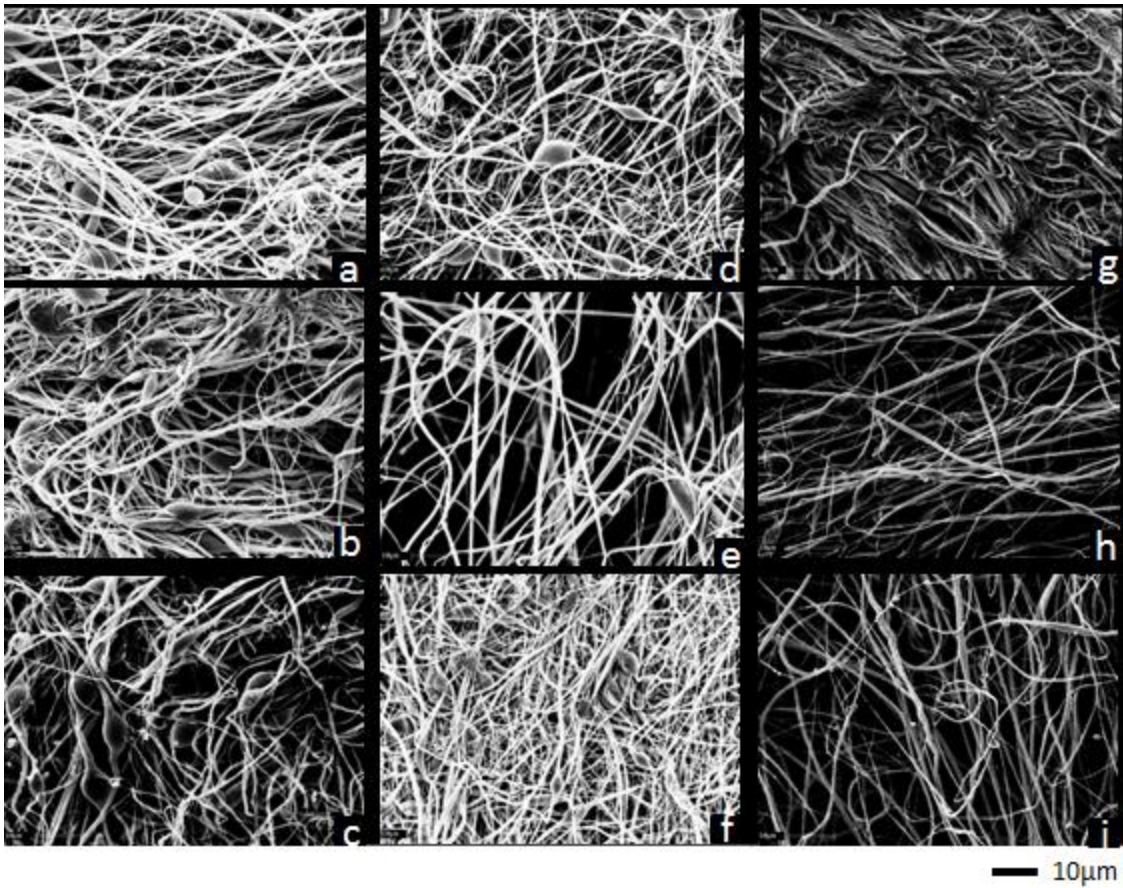


Figure 4.3. 5 SEM images of electrospun fibers from the solution of 12wt%PVDF with the solvent of 70v%acetone and 30v%DMAc spun at (a) 25°C (b) 40°C (c) 55°C and solvent of 80v%acetone and 20v%DMAc spun at (d) 25°C (e) 40°C (f) 55°C and solvent of 83v%acetone and 17v%DMAc spun at (g) 25°C (h) 40°C (i) 55°C with the condition of distance at 14cm, voltage at 15kV and flow rate of 0.05ml/min

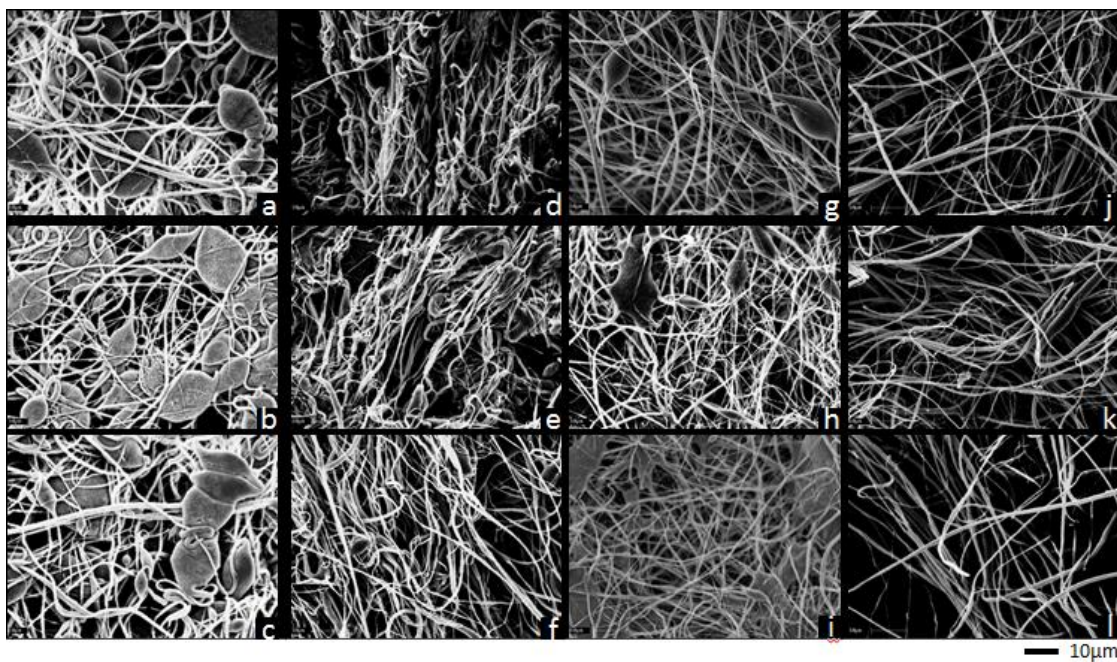


Figure 4.3. 6 SEM images of electrospun fibers from the solution of 14wt%PVDF with the solvent of 50v%acetone and 50v%DMAc spun at (a) 25°C (b) 40°C (c) 55°C and solvent of 80v%acetone and 20v%DMAc spun at (d) 25°C (e) 40°C (f) 55°C and solvent of 83v%acetone and 17v%DMAc spun at (g) 25°C (h) 40°C (i) 55°C and solvent of 86v%acetone and 14v%DMAc spun at (j) 25°C (k) 40°C (l) 55°C with the condition of distance at 14cm, voltage at 15kV and flow rate of 0.05ml/min

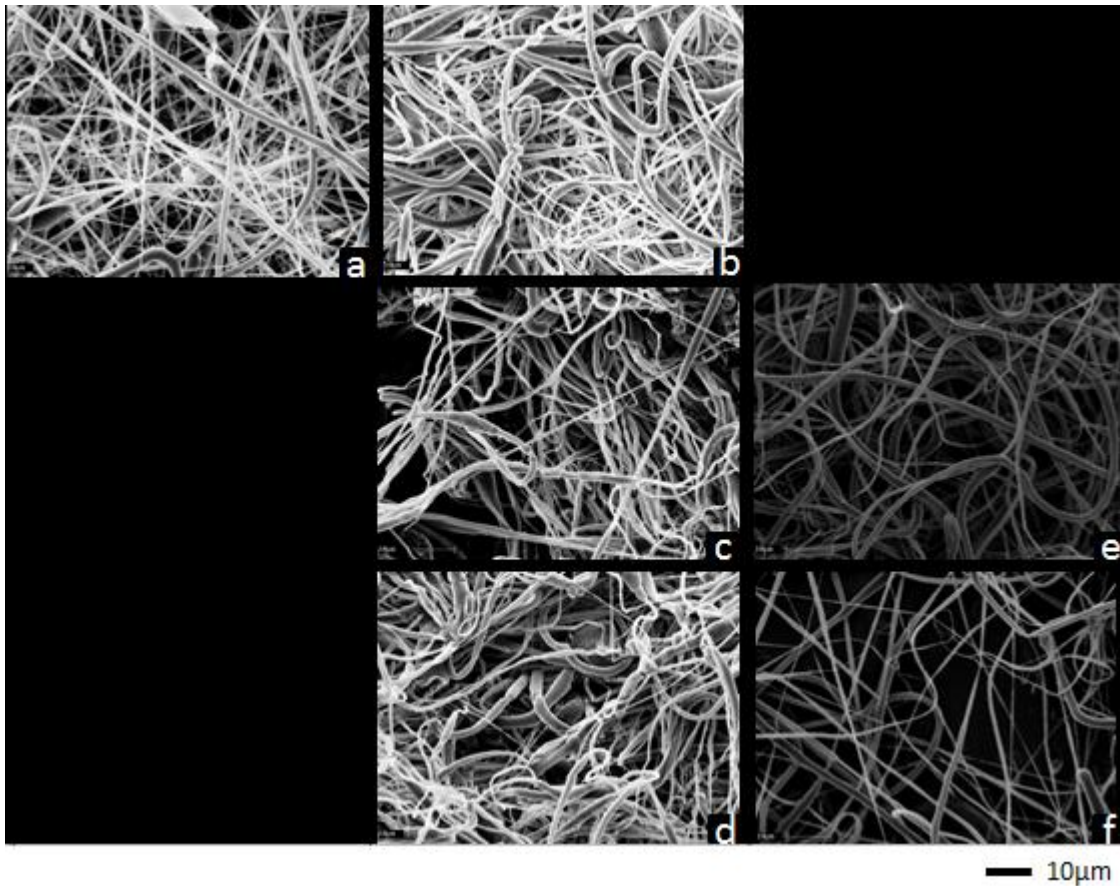


Figure 4.3. 7 SEM images of electrospun fibers from the solution of the 16wt%PVDF with solvent of 80v%acetone and 20v%DMAc spun at (a) 25°C with the condition of distance at 15cm, voltage at 15kV and flow rate of 0.06ml/min solvent of 83v%acetone and 17v%DMAc spun at (b) 25°C (c) 40°C (d) 55°C with the condition of distance at 14cm, voltage at 15kV and flow rate of 0.05ml/min solvent of 86v%acetone and 14v%DMAc spun at (e) 40°C (f) 55°C with the condition of distance at 14cm, voltage at 15kV and flow rate of 0.05ml/min

The fibers in figure 4.3.7 also proves that there is limitation exist for acetone to lower the viscosity. 83v%acetone is not adequate to lower the viscosity of 16wt%PVDF solution nor that concentration is not capable of slow the evaporation rate of that amount of acetone. Those two factors create the fibers with large diameters. However, as more acetone is added, the solution becomes viscous again and the amount is enough not to evaporate before whipping motion. Figure 4.3.8 shows distinguishable difference in fibers spun from various solvent compositions. When the volume percent of acetone is lower as 50%, the solution produces fine fibers but some beads also exist. When 20v% more acetone is added into the solvent, beads are no longer observed and fibers become straighter. Fibers in a shows that acetone is neither enough to make the solution viscous nor facilitate the electrospinning because the amount is small and evaporates faster than the effect of high concentration to slow the evaporation. Fiber morphology in b is improved but still it has large fiber diameter. 80v%acetone is enough to make the solution viscous and its evaporation rate is able to be decreased by the 18wt%concentration. However, the concentration is unable to slow the evaporation of more acetone and produces thicker fiber diameter as shown in d. Not all the images of the fibers were taken under the SEM since firstly obtained few images direct that fiber morphology is indifferent to different condition investigated and the crystallinity. Fiber diameter of each images have been measured and correlation with other results is plotted in figure 4.3.9.

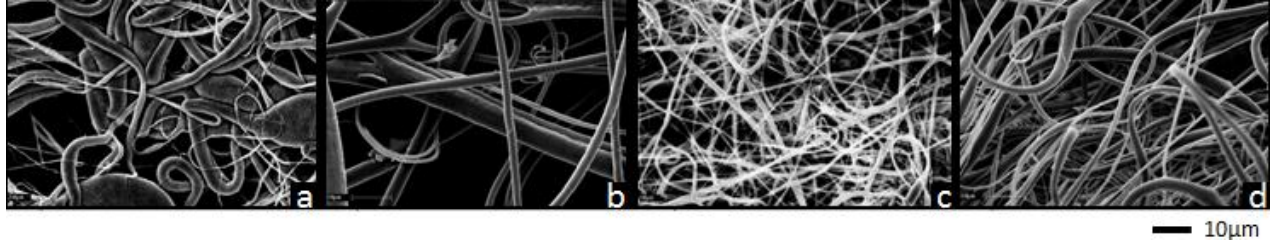


Figure 4.3. 8 SEM images of electrospun fibers from the solution of the 18wt%PVDF with the condition of distance at 14cm, voltage at 15kV and flow rate of 0.05ml/min  
 (a)solvent of 50v%acetone and 50v%DMAc spun at 25°C  
 (b)solvent of 70v%acetone and 30v%DMAc spun at 25°C  
 (c)solvent of 80v%acetone and 20v%DMAc spun at 25°C  
 with the condition of distance at 15cm, voltage at 15kV and flow rate of 0.06ml/min  
 (d)solvent of 83v%acetone and 17v%DMAc spun at 25°C

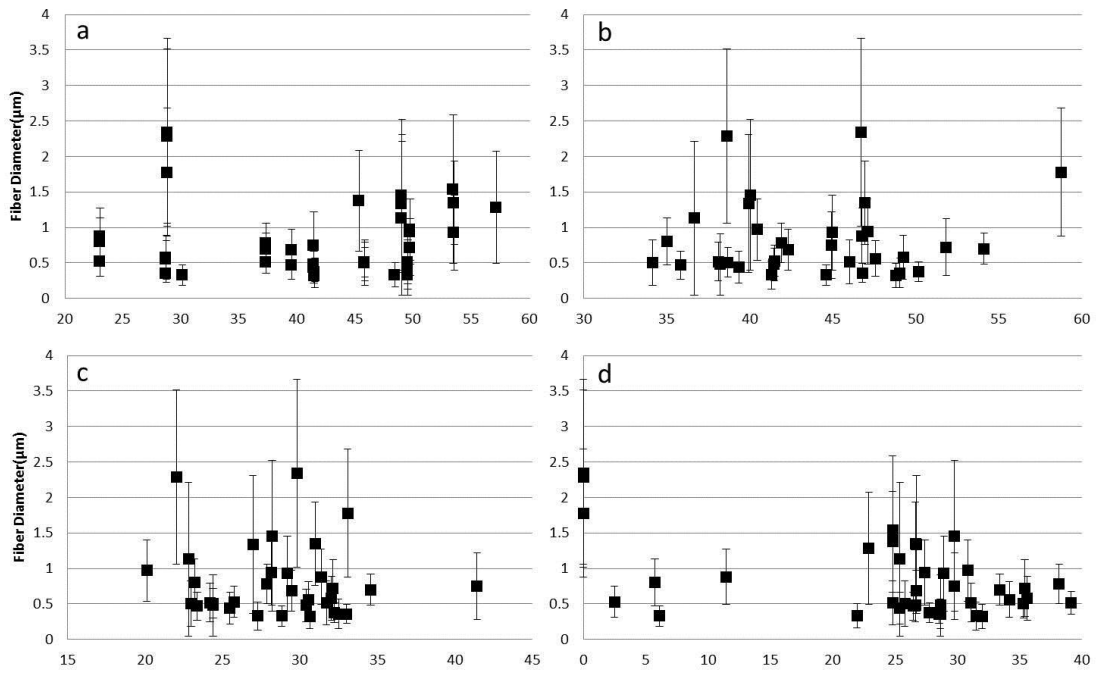


Figure 4.3. 9 Fiber diameter depending on a) PVDF concentration, b) total %crystallinity by XRD, c) %β crystallinity by XRD and d) total %crystallinity by DSC

Most samples have great variation from 10% to 680% of the mean of fiber diameter. In figure 4.3.9a fiber diameter is plotted against the PVDF concentration solely on DMAc as solvent. While acetone is a latent solvent which requires heat to dissolve PVDF, the reason for adding acetone in solvent is to facilitate the electrospinning process which will form better fiber, it is excluded. At 29%PVDF/ DMAc, the average fiber diameter becomes the largest but it varies even at the same concentration of PVDF. Thus, this approach is not necessary. The average fiber diameter reaches highest point twice when the total crystallinity measured by XRD is 38% total crystallinity and 47% total crystallinity. However, they do not have any pattern. For the % $\beta$  crystallinity measure by XRD, the average fiber diameter is maximized at 22%  $\beta$  crystallinity and 30%  $\beta$  crystallinity. These two points are related to highest fiber diameter with the total crystallinity. The samples for these points are 18wt%PVDF with the solvent of 50v%acetone and 50v%DMAc. The sample with lower crystallinity spun at 40°C and the other one spun at 25°C. However, for the plot with the total crystallinity by DSC the average fiber diameter is largest when the crystallinity is 0%. It does not have trend with total crystallinity by DSC. Overall, all four plots do not show particular correlations. Crystallinity will be related more likely with the orientation of the fibers rather than its thickness. Although fiber diameter is not necessarily related to the either total or  $\beta$  crsytallinity, the ones identified as high total and  $\beta$  crystallinity shows good fiber morphology with uniform fibers and less beads and without latent solvent left. In order to use in application, fibers should exhibit good

morphology and since fibers with high  $\beta$  crystallinity also shows good fiber morphology. Thus, no other combination of parameters needs to be investigated to improve fiber morphology. Nonetheless, as shown in figure 4.3.10, the fiber diameter has some closeness to the concentration although the influence of the concentration differs from sample to sample. When the concentration of the solution which later is spun to fibers increases, the fiber diameter generally increases although there are outliers. The fiber diameter of the fibers spun with the solvent whose volume percent of acetone is 80% at 40°C and 55°C, decreases at 14wt%PVDF. However, it becomes largest when the concentration is 18wt%PVDF. It proves that the fiber diameter increase with the concentration. Since higher concentration result in more viscous solution which forms larger Taylor cone then thinner jet. Because viscous solution has higher surface tension, higher voltage needs to be applied to pull the polymer into straight and uniform fibers. The increase is most dramatic when the volume percent of acetone in the solvent used to prepare the sample is 50v%. The solvent-non-solvent composition also has the effect over the fiber diameter since acetone should make the solution less viscous. However, when the concentration of polymer is so low that it cannot slow the evaporation of acetone, addition of acetone becomes meaningless. Also, if high temperature encourages acetone to be evaporated faster and it evaporates too early, it also becomes pointless. When the fibers are spun at 25°C, increase in acetone content in solvent results in decrease in fiber diameter due to decrease in viscosity. When the spinning temperature increases to 40°C, the trend varies

with the polymer concentration. The fiber diameter of 14wt%PVDF sample decreases with the acetone content and become steady after the volume percent of acetone in the solvent reaches 80v%. When the volume percent of acetone in the solvent is greater than 70v%, adding more acetone leads the greater fiber diameter for 16wt%PVDF and 18wt%PVDF samples. 18wt%PVDF sample spun at 55°C shows the same trend. The fiber diameter of 12wt%PVDF sample spun at both 40°C and 55°C, increase with acetone addition and when it becomes 80v%acetone, it has its maximum. After that, the fiber diameter decreases. Adding acetone has no influence over fiber diameter when 14wt%PVDF and 16wt%PVDF solutions are spun at 55°C because high temperature causes acetone to evaporate too fast. For some samples, 40°C is the critical spinning temperature. After that temperature, the fiber diameter spun from the solution of 12wt%PVDF mixed with the solvent of 80v%acetone and 20v%DMAc stop increasing and that from the solution of 14wt%PVDF and the solvent of 50v%acetone and 50v%DMAc stop decreasing. For sample spun from 14wt%PVDF with 50v%acetone in solvent, the fiber diameter increases till the spinning temperature reaches 40°C. This can be explained by early evaporation of acetone. Interestingly, it decreases afterward and this observation cannot be explained except for that 55°C is very close to the boiling point of acetone. If it boils while the solution is in the syringe, it might have changed the structure of the polymer solution. The fiber diameter is not affected by the spinning temperature when spun from 12wt%PVDF with solvent of 70v%acetone and 30v%DMAc, 12wt%PVDF with the solvent of 83v%acetone

and 17v%DMAc, 14wt%PVDF with the solvent of 83v%acetone and 17v%DMAc and 14wt%PVDF 86v%acetone and 14v%DMAc. The solution with the low concentration is hard to lower the evaporation rate of the solvent. Also, there is plenty of acetone to evaporate. Thus, it will evaporate well at room temperature and increasing spinning temperature will not assist evaporation. The fiber diameter of some samples with high concentration decreases when the temperature increases with the help of increased evaporation rate of acetone. Those are spun from all 18wt%PVDF solutions and 16wt%PVDF with the solvent of 86v%acetone and 14v%DMAc. 16wt%PVDF with the solvent of 83v%acetone and 17v%DMAc is the only solution to produce increasing diameter with the temperature. The solution also exhibits abnormal rheological data in chapter 4.2 and will be explained by the complicated combined effect of the polymer concentration, spinning temperature and the volume percent of acetone in solvent. Figure 4.3.11 show bigger trend of the fiber diameter depending on three variables. It suggests that the fiber diameter is mostly affected by the concentration. The spinning temperature and the volume percent of acetone in solvent do have some influence on fiber diameter as acetone supposed to facilitate electrospinning process with the advantage of rapid evaporation rate. However, the effects are not obvious. The results are also affected by the combination of the each parameter.

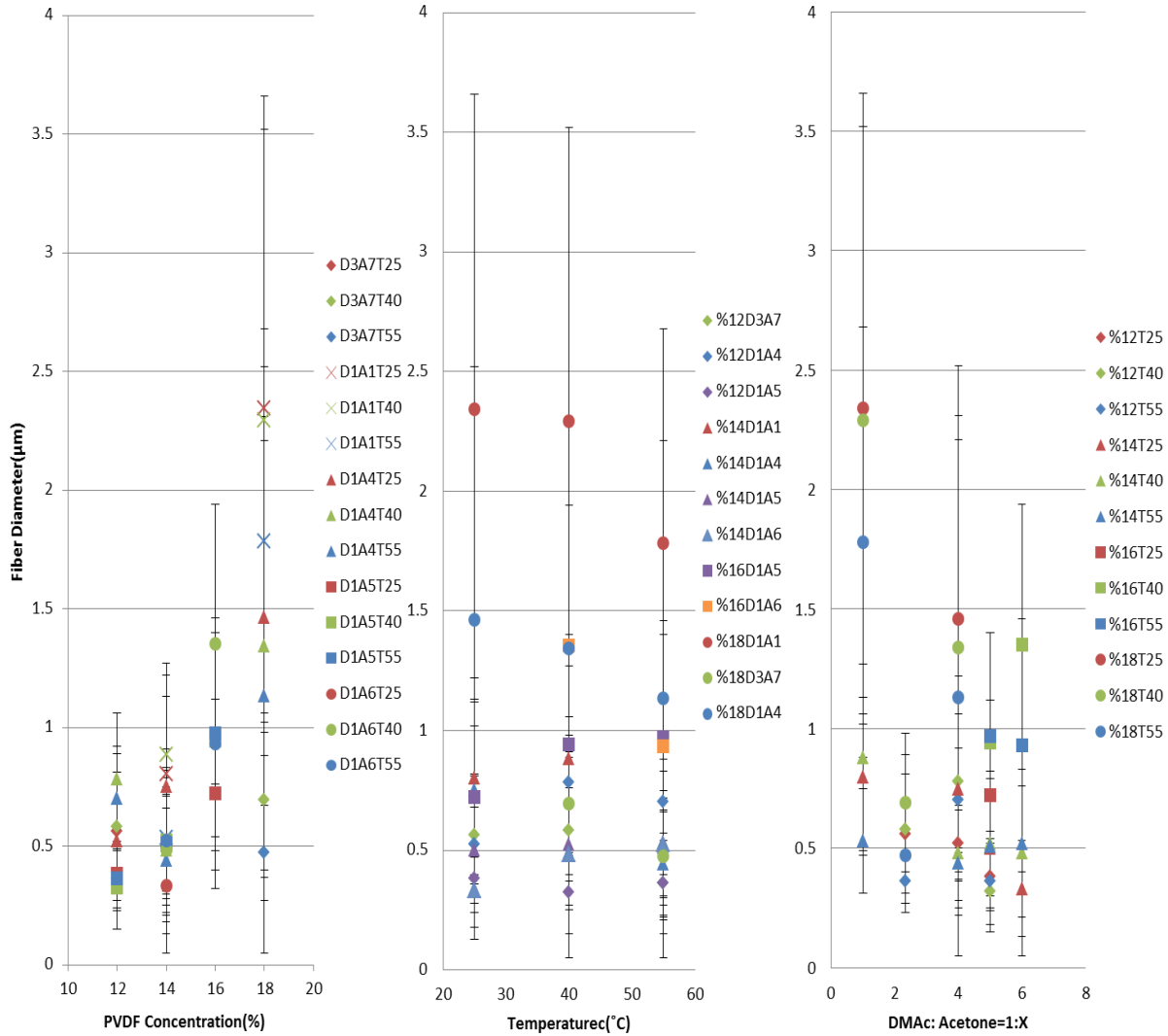


**Figure 4.3. 100 Fiber diameter(symbol) depending on PVDF concentration by wt%, the spinning temperature and the volume percent of acetone in solvent with the standard deviation(line with top and bottom)**

**\*D#=DMAC ratio to acetone, A#=Acetone ratio to DMAC, T#=Spinning Temperature, %#=PVDF concentration in wt%**

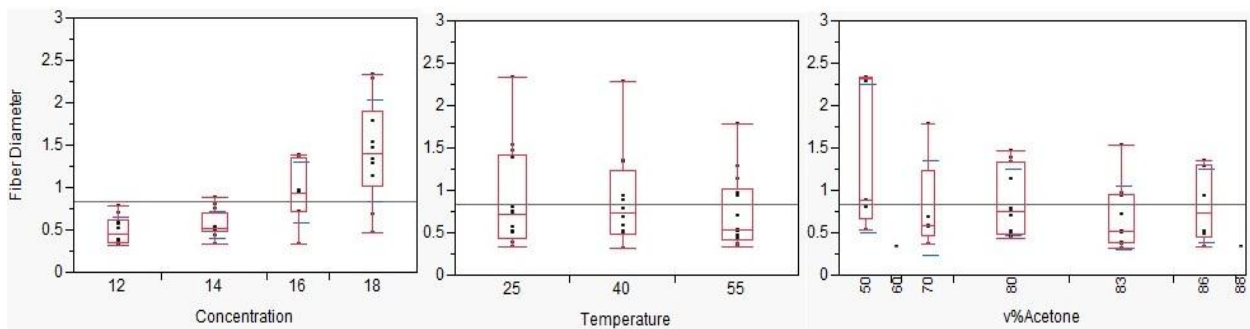


**Figure 4.3. 11 The trend of fiber diameter depending on PVDF concentration in wt% , the spinning temperature and the volume percent of acetone in solvent**

#### 4.4 Crystallinity and Crystalline Phases

Two different methods were used to measure the total crystallinity of the fiber, DSC and XRD. Interestingly, both results show the sharper peaks than the ones shown in literature. Figure 4.4.1.a is the heat flow of the PVDF pallet and 4.4.1.b is the heat flow exhibited by most of the samples obtained by DSC. However, some samples presented different behavior as shown in figure 4.4.1.c. In figure 4.4.2 heat flow on heating of all the samples with low volume percent of acetone in solvent plotted together so their base lines have been changed. These samples are spun from the solvent contains relatively low acetone as 50 or 60v%. Orange in the middle is for 80v%acetone and is added for the comparison. The samples spun from low acetone containing solution have enormous cold crystallization peak. It indicates that crystallization is occurring on heating the sample. Typically, because DSC measures the difference in crystallinity, if fibers have higher crystallinity to begin with, the peak is smaller than that for lower crystalline fibers which has potential to crystallize more. However, heat flows of cooling and reheating are similar to other samples. Noticeable difference between heating and reheating curves suggest that samples are changing during the process. Heat flow of fibers spun from 14wt%PVDF with the solvent of 80v%acetone and 20v%DMAc does not show distinguishable cold crystallization peak. Compared to 80v%acetone(1:4) one, while these samples spun with low volume of acetone in solvent have cold crystallization, they also have broader peak at melting point. Also, the minimum of those peak shifts. For example, for 50v%acetone(1:1), cold

crystallization peak moves to higher temperature as the spinning temperature increases. This might be that when fibers spun from the solution with low volume percent of acetone, higher temperature aids solvent to evaporate faster so it would have more crystallinity in fibers. Thus, in order to crystallize more, higher temperature is needed. However, 14wt%PVDF one does not concur since the cold crystallization peak for the sample spun at 55°C is larger and samples spun at lower temperature do not show apparent peak. This might be due to the crystallization from residual solvent. As shown in chapter 4.3, those samples had few spots of solvent. However, because increasing spinning temperature helps solvent to evaporate faster, less solvent is going to end up at collector with higher spinning temperature. That is the reason that the fibers from lower spinning temperature are more crystallized before so it does not crystallize during the DSC. The fibers spun from 60v%acetone has different trend. Cold crystallization peak does not shift for the samples from lower spinning temperature and the size of the peak and the melting points are similar. However, fibers spun at 55°C shows different trend and there is no clear explanation. The peaks of melting temperature are big and vague. However, when the minimum point is considered as melting point, it slightly shifts to the lower temperature with the increase of spinning temperature. The entire sample has lower melting point than the fibers spun from 80v%acetone do. Lower concentration spun at 55°C shows two peaks and they might represent different crystalline phases. All other samples not shown have similar peak positions and the difference is the height of the heat of fusion

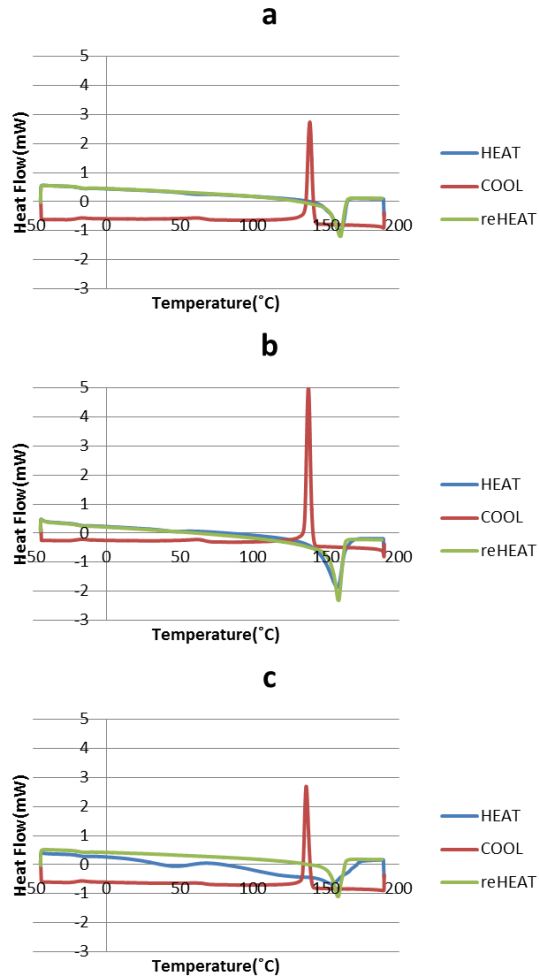


Figure 4.4. 1 a) PVDF Pellet b) 14wt%PVDF dissolved in solvent with 80v%acetone and 20v%DMAC  
 c) 14wt%PVDF dissolved in solvent with 50v%acetone and 50v%DMAC

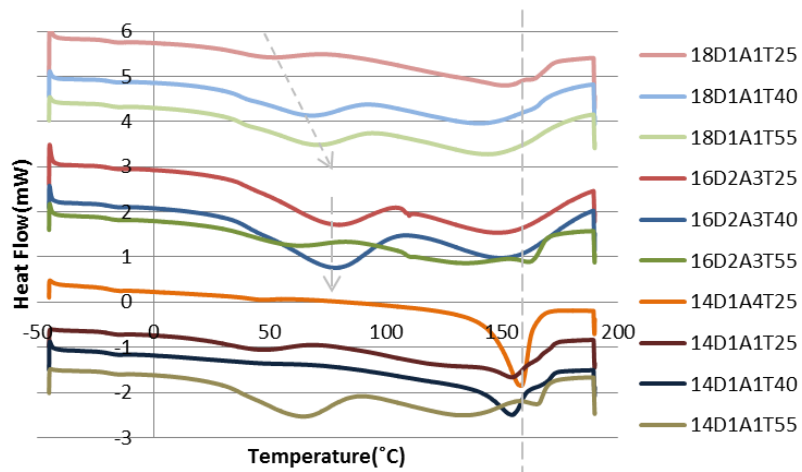
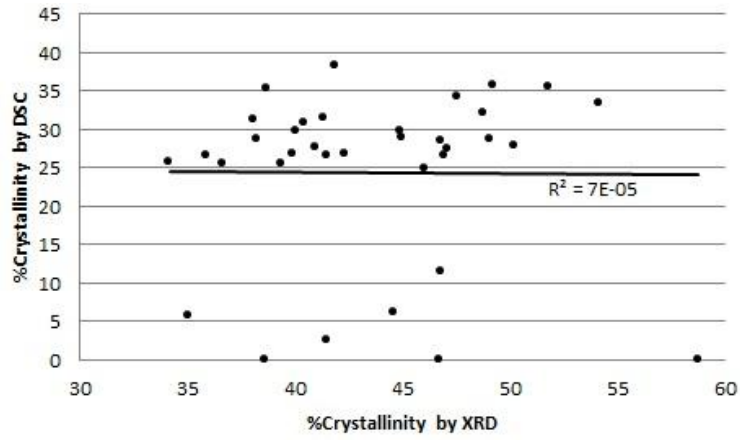
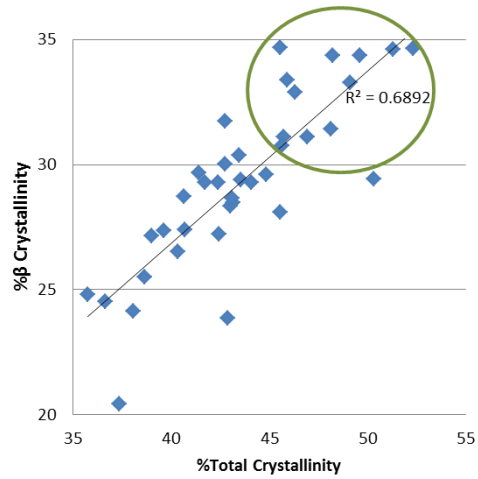


Figure 4.4. 2 Comparison of cold crystallization peak

peak which is used to calculate the total crystallinity comparing data at 100% crystallinity. Figure 4.4.3 shows the correlation of the total crystallinity between DSC and XRD and since the  $R^2$  value is very low, it can be concluded that there is no correlation between the two measurements. During the XRD measurement, the temperature remains steady but during the DSC, there is a great degree of temperature change and that explains the difference. However, theoretically, crystallinity measured from DSC should be higher but the result shows otherwise. This could be from wrong data of enthalpy of fusion at 100% crystallinity because the crystallinity calculated from that data based on difference in enthalpy of fusion. If the original data is low, the calculated crystallinity has to be low. For better comparison of data from these two methods, temperature dependent XRD could be used to mimic the DSC process. The decision is made that more promising total crystallinity is from XRD. XRD gives not only the total crystallinity but also percent crystallinity for each crystalline phase. When the sample is all crystalline, the peaks are narrow and sharp. However, as amorphous region increases the peaks become broader. Each peak represents different crystalline phases. The highest peak is located at the second after  $\alpha$  peak and it represents  $\beta$  crystalline phase. In order to maximize piezoelectric property, this  $\beta$  peak has to increase. Figure 4.4.4 suggests the correlation between the total crystallinity and the  $\beta$  crystallinity.  $R^2$  suggests some correlation between two and this means that for many cases piezoelectric property can be increased when the total crystallinity increases. The green circle indicates the conditions can maximize total and  $\beta$  crystallinity.



**Figure 4.4. 3** No correlation was found between % total crystallinity determined by DSC and XRD



**Figure 4.4. 4** A weak correlation between total crystallinity and β crystallinity. In several cases fibers with high β crystallinity were produced.

Those conditions are listed in Table 4.4.I. No overall trend to maximize crystallinity for any single variable was found but rather specific sets of composition and temperature conditions. Within subsets of the data, trends could be identified. High crystallinity was achieved at higher spinning temperatures with constant PVDF concentration and solvent composition. It is highly probable that the high crystallinity is related to evaporation rate of the solvent. In order to exhibit piezoelectric properties,  $\beta$  crystallinity is required and better piezoelectric properties higher %  $\beta$  crystallinity is needed. However, it is also important to have good fiber morphology in order to be used in other applications. Although the conditions in table 4.4.I are not necessary to form fibers with the best morphology, as shown in section 4.3, all fibers spun under these conditions exhibit good fiber morphology. They have neither beads nor solvent left and the fibers are uniform. For samples in figure 4.4.5 with concentration of 12wt%PVDF, the amount of  $\beta$  crystalline phase increased with the amount of acetone added. Change in the amount of  $\alpha$  crystalline phase varies with the ratio of acetone as well. Those results can be explained by dependence of the formation of each crystalline phase on the evaporation rate. With solvent of 20v%DMAc and 80v%acetone (1:4),  $\beta$  crystallinity increases with the spinning temperature.  $\alpha$  phase increases at the same time. Thus,  $\beta$  crystallinity can be increased not only by increasing the volume percent of acetone in solvent but also by spinning at higher temperature. Both acetone and temperature increase solvent evaporation rate.

**Table 4.4. I Combinations to maximize both total and  $\beta$  crystallinity**

Concentration(wt%)	Acetone(v%)	Temperature( $^{\circ}$ C)
12	80	55
12	83	25
12	83	55
14	80	25
14	80	40
14	86	25
14	86	55
16	60	25
16	60	40
18	70	25
18	70	55
18	80	55

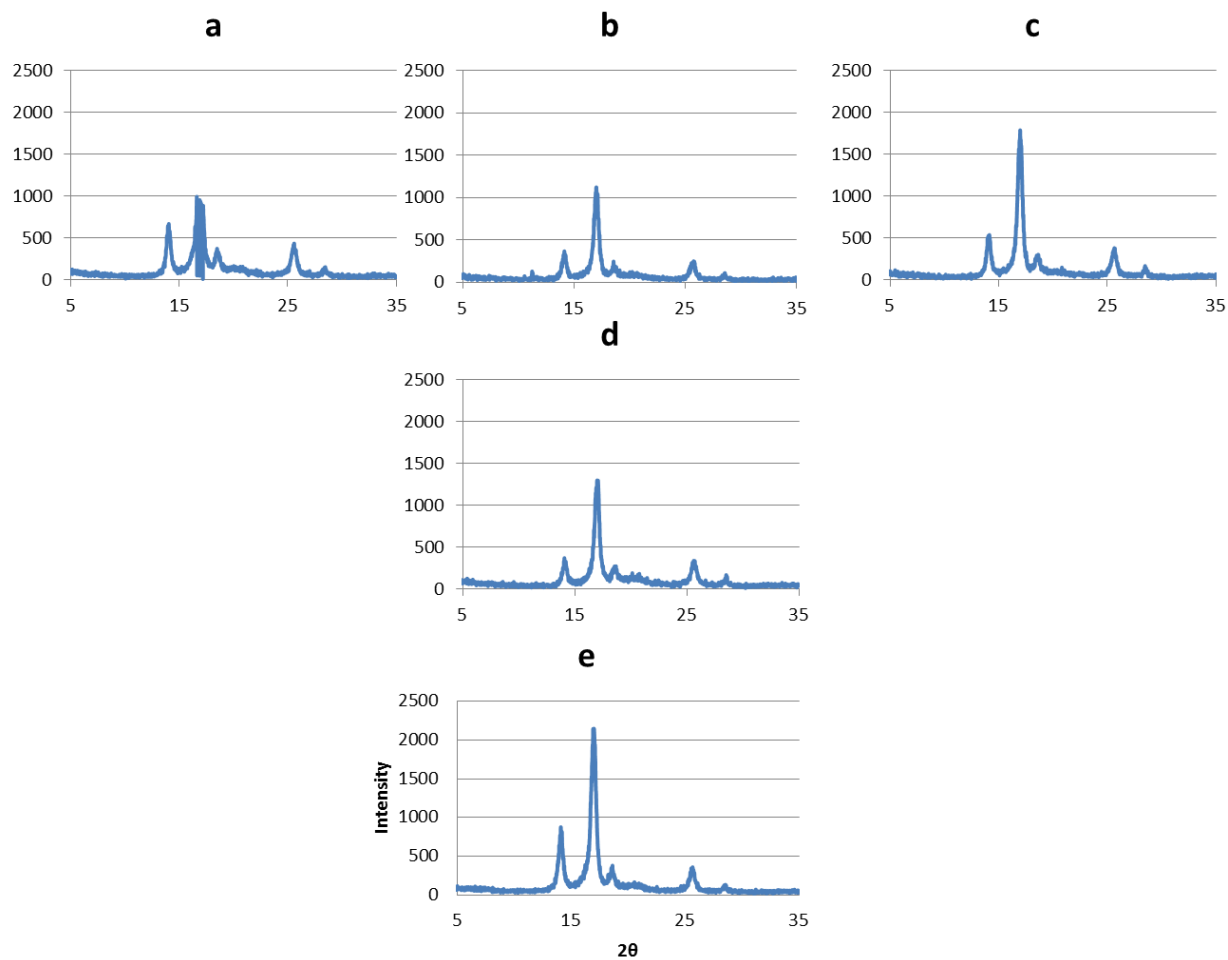


**Figure 4.4. 5** 12wt%PVDF at 25°C with solvent of a) [70v%acetone+30v%DMAc] b)[80v%acetone+20v%DMAc] c)[83v%acetone+17v%DMAc] and d) [80v%acetone+20v%DMAc] at 40°C e) [80v%acetone+20v%DMAc] at 55°C

For samples in figure 4.4.6 with 14wt% of PVDF, the effect of acetone and the temperature does not show nice trend. For each low spinning temperature is the same and right side obtains more volume percent of acetone in solvent. First row suggests that adding acetone might increase or decrease  $\beta$  crystallinity of samples spun at 25°C. However, second row which spun at 40°C show that  $\beta$  crystallinity is inversely proportional to the amount of acetone in solvent. Finally, on third row the acetone does not have any influence on  $\beta$  crystallinity and this is because at 55°C, temperature has more effect on solvent evaporation than the acetone has. Each column has the same solvent system and bottom has higher spinning temperature. First column suggest that the raising spinning temperature might increase or decrease the  $\beta$  crystallinity. On the other hand, higher spinning temperature can result in low  $\beta$  crystallinity as seen in second column and this could be due to greater influence of quenching effect. Lastly, third column shows no apparent dependence on spinning temperature and this can be explained by the greater impact of acetone on solvent evaporation than temperature. Furthermore, it can be concluded that when one variable reaches its optimum point, the other variable shows no or little effect on crystallinity.

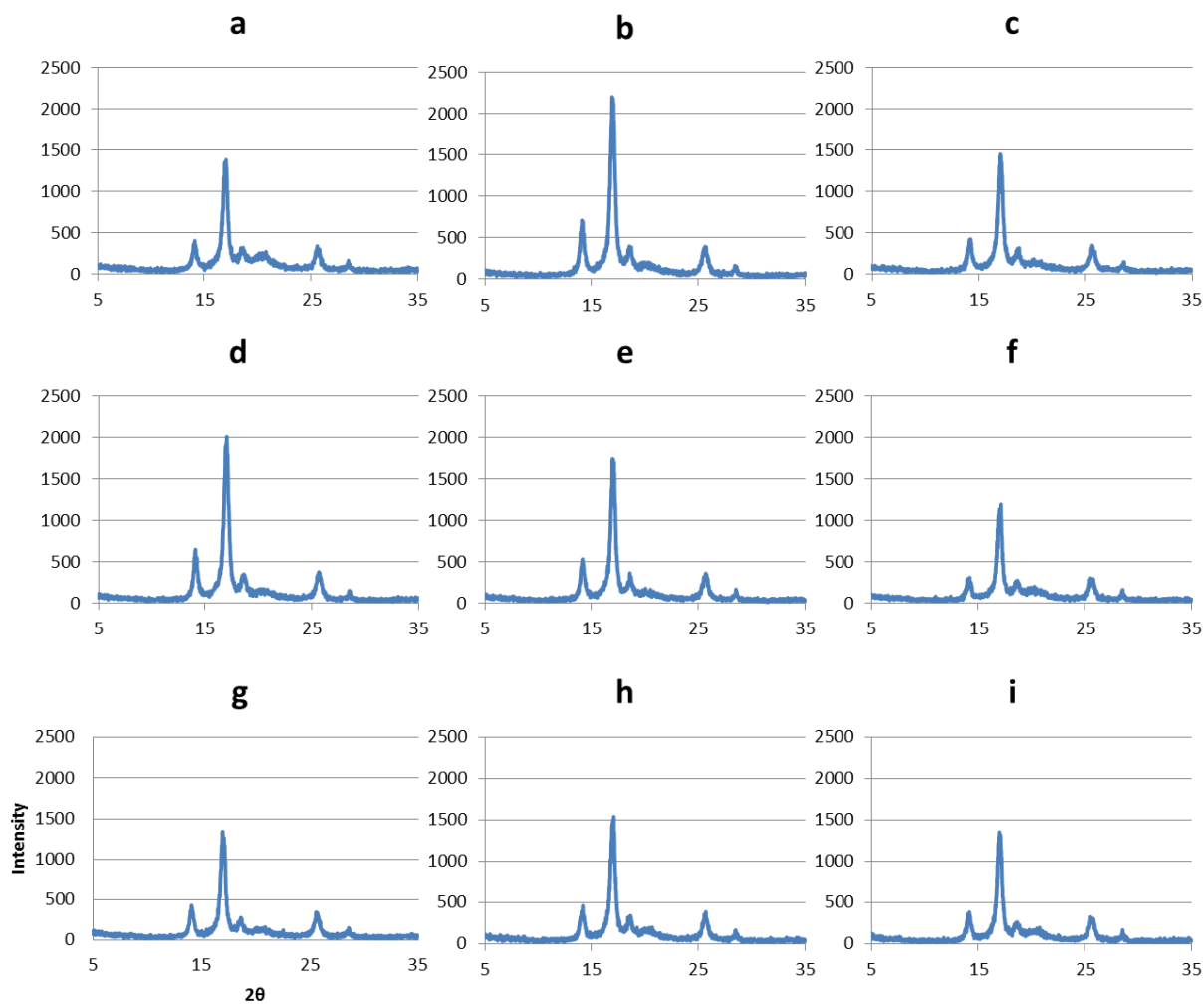
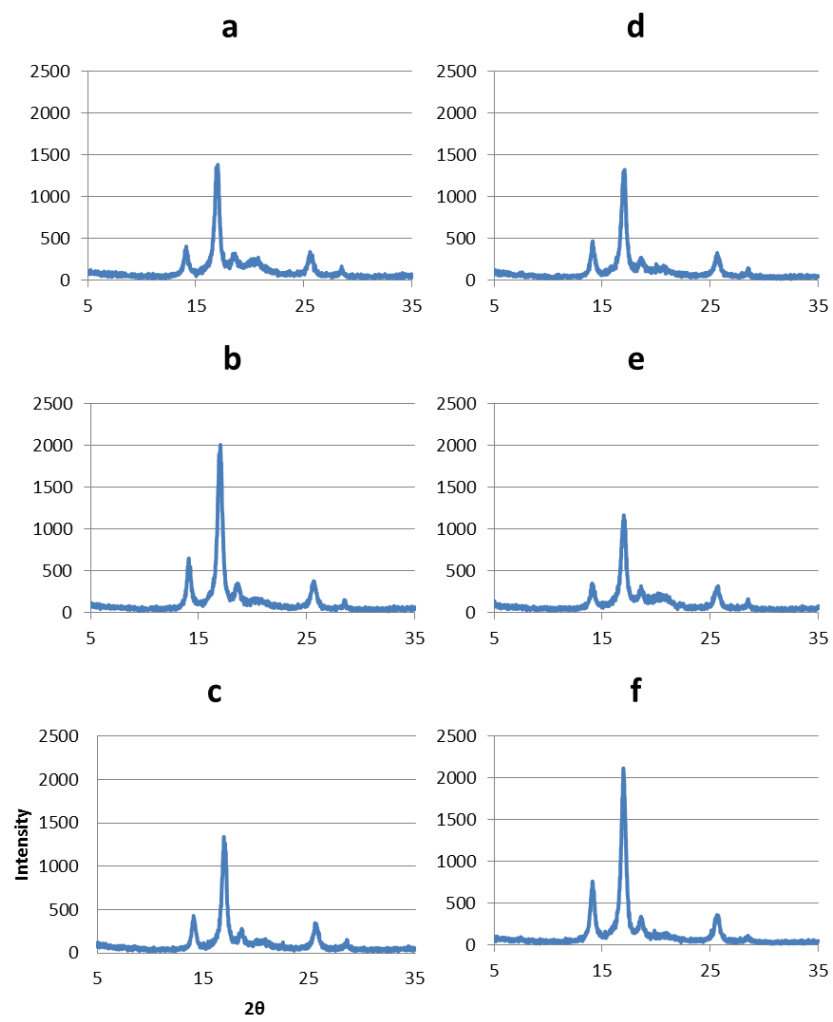


Figure 4.4. 6 14wt%PVDF at 25°C with solvent of a)[50v%acetone+50v%DMAc] b)[80v%acetone+20v%DMAc] c)[83v%acetone+17v%DMAC] at 40°C d)[50v%acetone+50v%DMAc] e)[80v%acetone+20v%DMAc] f)[83v%acetone+17v%DMAC] at 55°C g)[50v%acetone+50v%DMAc] h)[80v%acetone+20v%DMAc] i)[83v%acetone+17v%DMAC]

In figure 4.4.7, solvent system is kept at 50v%acetone and 50v%DMAc and each row represents the different spinning temperature. When fibers spun at 25°C, concentration does not have any influence on  $\beta$  crystallinity and this might be because at lower spinning temperature and lower volume percent of acetone, the effect of concentration is too weak to change the evaporation rate of solvent. Usually, solvent evaporates faster at low concentration. However, second row shows that increase in concentration greatly decrease  $\beta$  crystallinity. High concentration slows the evaporation of solvent. However, the SEM images of these samples suggest otherwise because 14wt%PVDF is the one has solvent left in fibers after the spinning. The residual solvent might have increased the  $\beta$  crystallinity of the fibers. However, unexplained part is that since temperature should help the evaporation of the solvent so there should be less solvent left on the collector after the spinning. Thus, the crystallinity should be higher for those spun at lower temperature. However, it does not show that although it is low for fibers spun at 55°C. At that spinning temperature, increase in concentration helps to form more  $\beta$  crystallinity as shown in third row. Concentration positively or negatively affects forming  $\beta$  crystallinity depending on the spinning temperature. Figure 4.4.8 again proves the complexity of combined effect of polymer concentration, spinning temperature and the volume percent of acetone in solvent. However, it also suggests different ways to maximize the  $\beta$  crystallinity. b, c and g have similar height of  $\beta$  crystalline phase peak although their concentration and spinning temperature are different.



**Figure 4.4. 7 with solvent of 50v%acetone and 50v%DMAc and 14wt%PVDF spun at a)25°C b)40°C c)55°C and 18wt%PVDF spun at d)25°C e)40°C f)55°C**

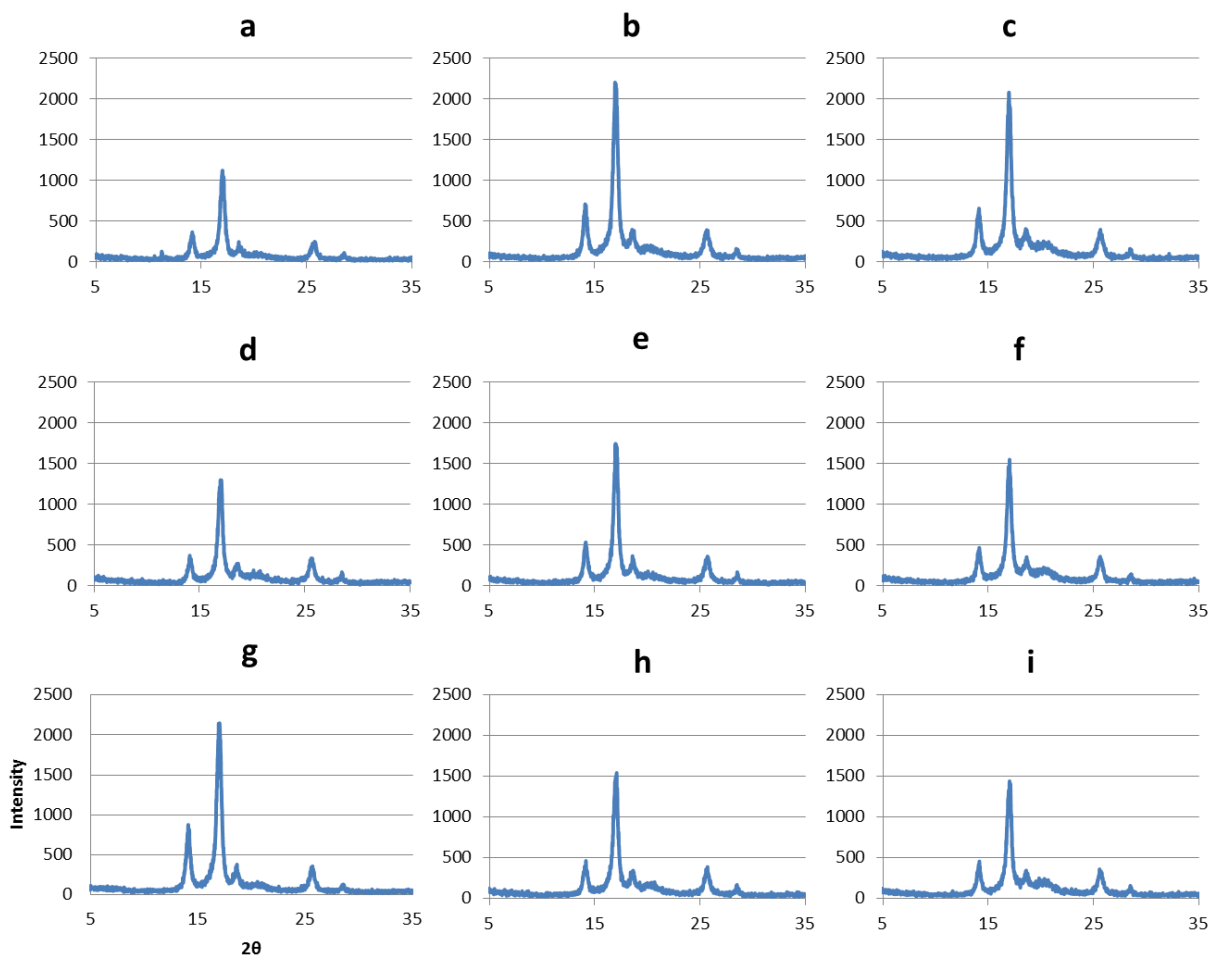


Figure 4.4. 8 with solvent of 80v%acetone and 20v%DMAc, spun at 25°C with a)12wt%PVDF b)14wt%PVDF c)18wt%PVDF and at 40°C d) 12wt%PVDF e)14wt%PVDF f)18wt%PVDF and g)12wt%PVDF h)14wt%PVDF i)18wt%PVDF

Thus, those three variables act favorably and unfavorably forming the  $\beta$  crystalline phase depending on other two variables. Figure 4.4.9 shows trends of  $\beta$  crystallinity of all the samples and its dependence on concentration, spinning temperature and the volume percent of acetone in solvent. It proposes that lower concentration is more likely form  $\beta$  crystallinity. The effect of spinning temperature is not great but it does suggest that 25°C is slightly better temperature to produce  $\beta$  crystalline phase and its wide range at 55°C suggests more dependence on concentration and the volume percent of acetone. It also shows that the optimum volume percent of acetone is 80v% for most of the sample but wide range of  $\beta$  crystallinity at that point also proves more reliance on other parameters, the concentration and the spinning temperature. In figure 4.4.10, the trend of total crystallinity is similar to that  $\beta$  crystallinity. However, it does show that more crystallinity at 18wt%PVDF.

The several conditions to increase % $\beta$  crystallinity have been identified. These conditions producing fibers with high % $\beta$  crystallinity are also capable of spinning uniform and less beaded fibers although there is no correlation between fiber diameter and the crystallinity. While connection between all three variables creates complicated effect on forming  $\beta$  crystallinity, the result also points that there are many different ways to achieve high % $\beta$  crystallinity. Not only two or all factors can work together to create more  $\beta$  crystalline phase but also individual factor can change the amount when other two factors are fixed. When one of the parameter is fixed, changing either of remaining ones can produce the same level of the  $\beta$  crystallinity.

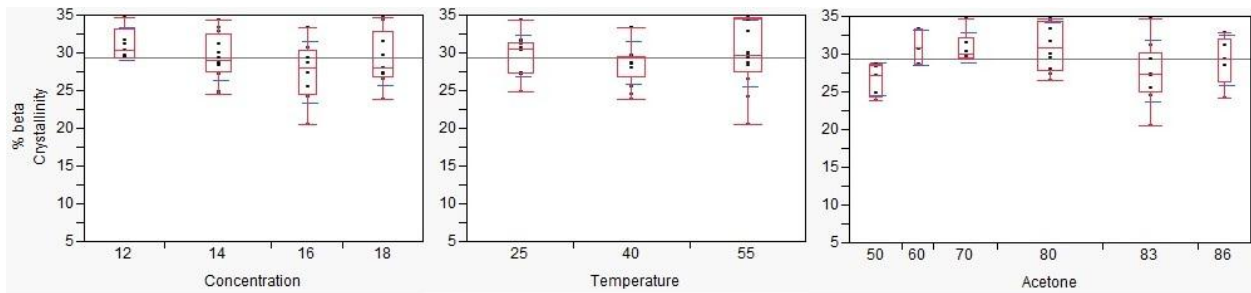


Figure 4.4. 10 Change in  $\beta$  crystallinity depends on concentration, spinning temperature and the volume percent of acetone

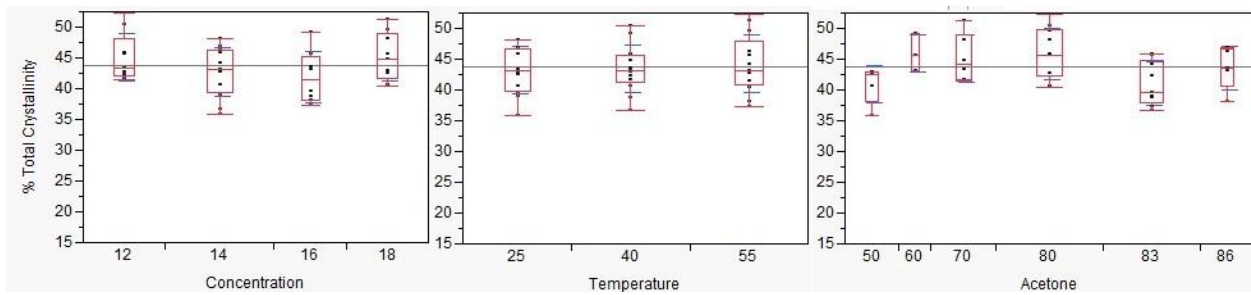


Figure 4.4. 9 Change in total crystallinity depends on concentration, spinning temperature and the volume percent of acetone

## 4.5 Statistical Analysis

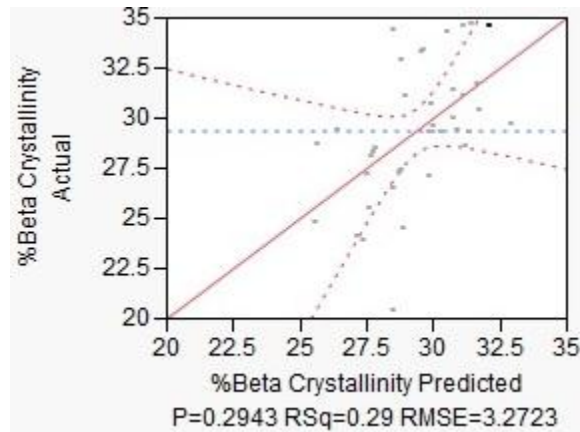


Figure 4.5. 1 Weak correlation between predicted and actual % $\beta$  crystallinity

In figure 4.5.1, % $\beta$  crystallinity has been predicted based on the experimental data. The prediction is calculated by the effect of the concentration of PVDF, spinning temperature and volume percent of acetone in solvent and as well as their combined effect. The three variables are not independent as electrospinning process is affected by the solvent evaporation rate and viscosity. Acetone is a volatile solvent with a low flash point which evaporates well even at room temperature. The evaporation rate increases with the temperature increase. Moreover, the evaporation rate is also influenced by the concentration. Solvent evaporates faster when the PVDF concentration of the solution is low. The evaporation of the solvent is also responsible for forming different crystalline phases.  $\beta$  phase preferably formed with low evaporation rate and  $\alpha$  phase with high rate and  $\alpha$  and  $\beta$  phase coexist with intermediate rates.<sup>16</sup> Since there was greater number of combination of variables than the sample size, the model has only 30% of accuracy as  $R^2$  value is 0.29. However,

p value suggests that it cannot reject null hypothesis so this is adequately fitted model. Table 4.5.I shows the p value for each variables and the combined effect. Lower p value suggest better fit model and higher p value means that the variable is less associated with the response. Concentration and the volume percent of acetone in solvent have more influence over the fit model than temperature does. Furthermore, the combined effect of the concentration and the spinning temperature is not counted largely for this fit model. No single variable or variable pair is significant at 95% confidence.

**Table 4.5. I p value for each effect and their connected effect on predicting % $\beta$  crystallinity**

Variables and Combinations	p
Concentration	0.15
Temperature	0.67
Acetone	0.15
Concentration&Acetone	0.26
Concentration&Temperature	0.83
Acetone&Temperature	0.58

Figure 4.5.2 shows the predicted trend of % $\beta$  crystallinity with combination of three variables. Since all three variables and the response cannot be plotted at the same time due to the limitation of the dimension, one variable, temperature, is fixed for each plot. First plot is at 25°C, second at 40°C and third at 55°C. In figure 4.5.3 there are plots of behavior of the % $\beta$  crystallinity according to experimental data. As the model can predict only 30% of the % $\beta$  crystallinity, model in figure 4.5.2 and plot of real data in figure 4.5.3 have some difference.

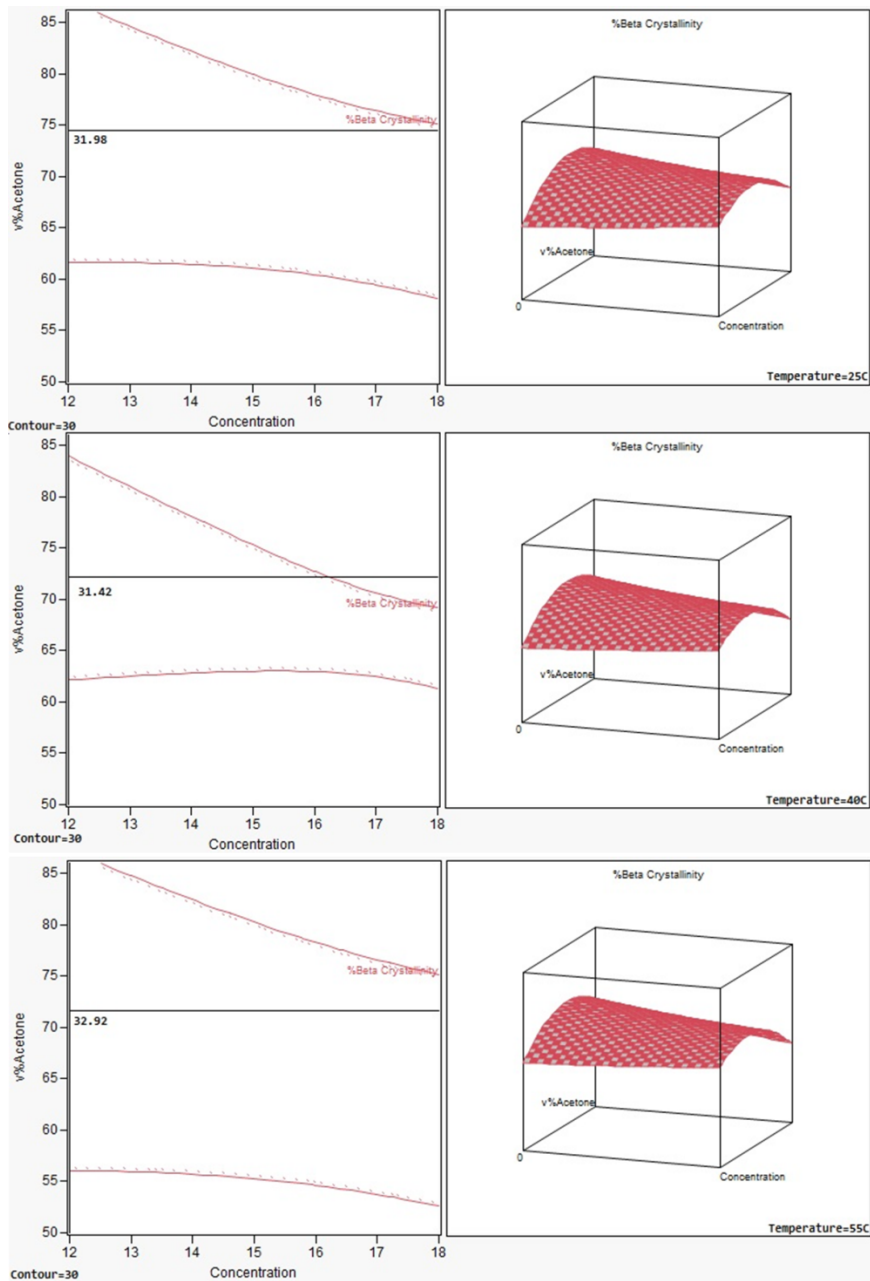


**Figure 4.5. 2 Plot of model to predict % $\beta$  crystallinity to respond to the combined effect of PVDF concentration and volume percent of acetone in solvent at 25°C, 40°C and 55°C from the top-Left: number in the middle is the highest predicted % $\beta$  crystallinity and area in the middle shows conditions to produce % $\beta$  crystallinity, Right: different combination (Acetone and Concentration) produces different level of % $\beta$  crystallinity(z)**

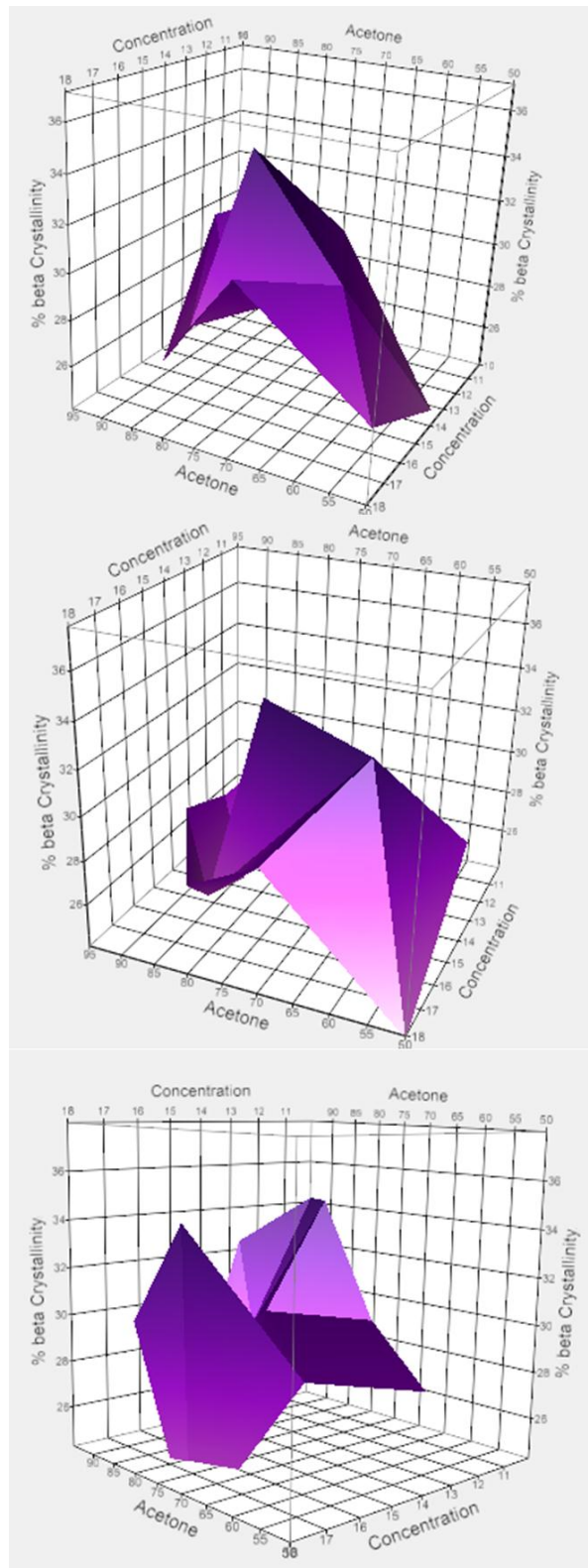


**Figure 4.5. 3** Plot of obtained % $\beta$  crystallinity from experiment depending on the combination of PVDF concentration and volume percent of acetone in solvent at 25°C, 40°C and 55°C from the top

The plots show the combined effect of PVDF concentration in solution and the volume percent of acetone present in solvent. The shapes of all three plots are different and this indicates that the combined effect of both parameters on %  $\beta$  crystallinity vary significantly with the temperature. When the fibers are spun at 25°C, it has one highest peak where the concentration is 14wt% and the acetone is 80v%. However, when the spinning temperature increases to 40°C, it has broad peak which seems to proportional line between the concentration and acetone parameters. The end points of the peak are 14wt%PVDF with 80v%acetone and 16wt%PVDF with 60v%acetone. Lastly, at the spinning temperature of 55°C, there are two peaks to represent maximized % $\beta$  crystallinity. One is broad peak whose end points are 12wt%PVDF with 80v% and 83v%acetone. The other peak is created by 18wt%PVDF and 80v%acetone. Thus, at 25°C, there exists only one condition to maximize % $\beta$  crystallinity. However, when the spinning temperature increases, few options become available. At 55°C, 80v%acetone is optimal for both low and high concentration. This indicates that at high spinning temperature with optimal acetone amount, concentration does not have influence on  $\beta$  crystalline phase formation. Since 40°C is rather complicated procedure to identify optimal condition to increase % $\beta$  crystallinty and only two conditions are found in table 4.4.I, it is better to use 25°C or 55°C for the spinning temperature. At 25°C, one can try high acetone percentage with low polymer concentration in solution. Acetone evaporates faster with low polymer concentration so more acetone is required.

However, when the concentration increases, it can slow the evaporation and less acetone is needed. Nevertheless, if high concentration makes the solution too viscous, more acetone will help to spin fibers during the electrospinning. The simplest way is to use 55°C as spinning temperature. Table 4.4.I shows all the concentration except for 16wt% whose crystallinity study is not investigated showing high % $\beta$  crystallinity. Thus, at this temperature, after identifying the optimal volume percent of acetone in solvent, several concentrations can be tried. As stated earlier, the conditions to maximize % $\beta$  crystallinity also exhibit good fiber morphology. Thus, the research can be focused to identify the condition to increase % $\beta$  crystallinity.

Table 4.5.II is a result from a simulation of 10,000 run with concentration(Mean:15wt%, SD:2), spinning temperature(Mean:40°C, SD:8) and v%Acetone(Mean: 70v%, SD:10) and it only includes the ones have higher % $\beta$  crystallinity than experiment results. Both plot and simulation suggest that lower concentration(<~14wt%) and 65~75v% of acetone tend to form  $\beta$  crystalline phase favorably. However, the simulation suggests that the temperature to be higher than the boiling point of the acetone to form more  $\beta$  phase. Although the boiling point of acetone may rise because of the interaction with other molecules in solution, it is hard to know its exact point. Moreover, It is unknown that if the acetone boils first or the whole solution acts together. Thus, it is not safe to go above the boiling point of the acetone as it might change the properties of the solution during the electrspinning. However, it is true that the solvent in the solution with lower concentration of polymer

evaporates faster and higher temperature improves evaporation as well. Furthermore, adequate amount of solvent is needed as all solvent has to evaporate before the jet reaches the collector in short time. If the solvent reaches at collector, the residual solvent affects the crystallinity of the fibers as it evaporates. In fact, the data might be resulted from that effect is not excluded nor identified so the model might be affected by those experiment data. Other reason for the importance of the amount of solvent and its evaporation rate is that if the amount is too low or the temperature is too high, all the solvent might evaporate before the solution becomes jet. Then, there is no benefit of using solvent to produce fibers during the electrospinning process. All the solvent has to evaporate during the whipping motion and identifying the amount of solvent at different concentration of polymer and spinning temperature is complicated. Both concentration and spinning temperature affect the evaporation of the solvent. Also, interaction between the different solvents, in this case good solvent and latent solvent, cannot be neglected. It is possible to predict % $\beta$  crystallinity for these factors and their interactions using surface response. However, in this case, the accuracy of the model is not high but more precise prediction can be made with more sample data.

**Table 4.5. II Conditions to create highest %  $\beta$  crystallinity from a simulation after 10,000 run**

Concentration(wt%)	Temperature( $^{\circ}$ C)	v%Acetone	% $\beta$ Crystallinity
12.29	64.20	69.66	34.68
12.25	64.37	72.41	34.71
14.56	67.56	66.27	34.71
9.68	62.57	75.10	35.74

## CHAPTER 5

### CONCLUSIONS

The concentration of PVDF, the volume percent of acetone in solvent and the spinning temperature have individual effect on fiber morphology, crystallinity and the formation of crystalline phases. Moreover, there exists interconnected influences and this connected effect is caused by the acetone which changes viscosity of the solution and evaporation rate of the solvent during the electrospinning. Acetone is capable of decrease viscosity but its capability may be limited by polymer concentration. The evaporation rate of acetone can be slowed by increase in polymer concentration but each concentration also its ability has limitation to the amount of acetone. Nevertheless, the temperature always increases the evaporation rate although there is competition with the effect of concentration which decreases the evaporation rate. Competition between two effects depends on the amount of acetone. Despite the complex relationship between the variables, rheology study proves the effect of acetone on viscosity of the solution and change in evaporation rate influence by the concentration and the temperature. The study of 18wt%PVDF with 86v%acetone and 14v%DMAc also shows that the viscosity increases with decrease in temperature and increase in time. No gelation during that time states that the gelation takes much longer than electrospinning span. No correlation between fiber diameter and viscosity is explained by the role of acetone during the electrospinning. High storage modulus which represents

entanglement density and its decrease with temperature describes unspinnability of solution of 18wt%PVDF with 86v%acetone and 14v%DMAc at lower temperature. The solution exhibit shear thinning behavior and the viscosity and chain entanglement depend on solution composition. Rheology study is important factor in spinning behavior. Acetone is added to facilitate the electrospinning with advantage of lowering spinnable polymer concentration by decreasing viscosity of the solution while increasing concentration over good solvent, DMAc. Furthermore, in order to produce fibers with good morphology and high crystallinity, the solvent should evaporate during the jet from needle tip to collector. On one hand, if the solvent evaporates too slow, solvent will be left on the collector along with fibers and may melt the fibers or change the crystallinity during evaporation. On the other hand, if the solvent evaporates too fast, it will produce thicker and ununiformed fibers. Increase in concentration always results in increase in fiber diameter. However, it also decreases the number of beads. The influences of the volume percent of acetone and temperature on fiber diameter are connected. High volume percent of acetone creates best fiber morphology but it does not necessarily have high  $\beta$  crystallinity which is responsible for piezoelectric properties. The total crystallinity has been found by DSC and XRD and  $\beta$  crystallinity has been identified by XRD. There is no correlation between two methods. The solution with low amount acetone(<60v%) shows large cold crystallization peak during DSC indicating that fibers did not crystallized during the electrospinning due to low evaporation of the solvent.

These peaks shift to higher temperature with increase in spinning concentration. During analyzing XRD data, there has been found weak correlation between the %total crystallinity and % $\beta$  crystallinity. Thus, fibers with high %crystallinity could possess high % $\beta$  crystallinity as well. By investigating three parameters and their interconnectivity, the combinations to maximize % $\beta$  crystallinity have been identified. It is also confirmed that those conditions produce good fiber morphology with uniform fibers with less beads. The connected effect of acetone and the concentration at different temperature have been investigated. The response of % $\beta$  crystallinity to combined effect of those two parameters significantly varies with the spinning temperature. At lower temperature, only one condition(14wt%PVDF and 80v%acetone) can produces maximum % $\beta$  crystallinity. As the temperature increase, more combinations become available but each concentration has different ideal v%acetone. Rather simplest way is to use high spinning temperature. At this point, one optimal volume percent of acetone(80v%) exists so several concentration can be tried even lower concentration as the model prediction suggested. Although this study suggests that many different ways to achieve high % $\beta$  crystallinity exist and identifies conditions to maximize % $\beta$  crystallinity, the value is not higher comparing to other literature. However, by using fibers spun under these conditions which also form good fiber morphology, % $\beta$  crystallinity can be increased more using further treatment such as annealing under tension. Finally, these fibers with good morphology and improved piezoelectric properties can be used in many applications.

## CHAPTER 6

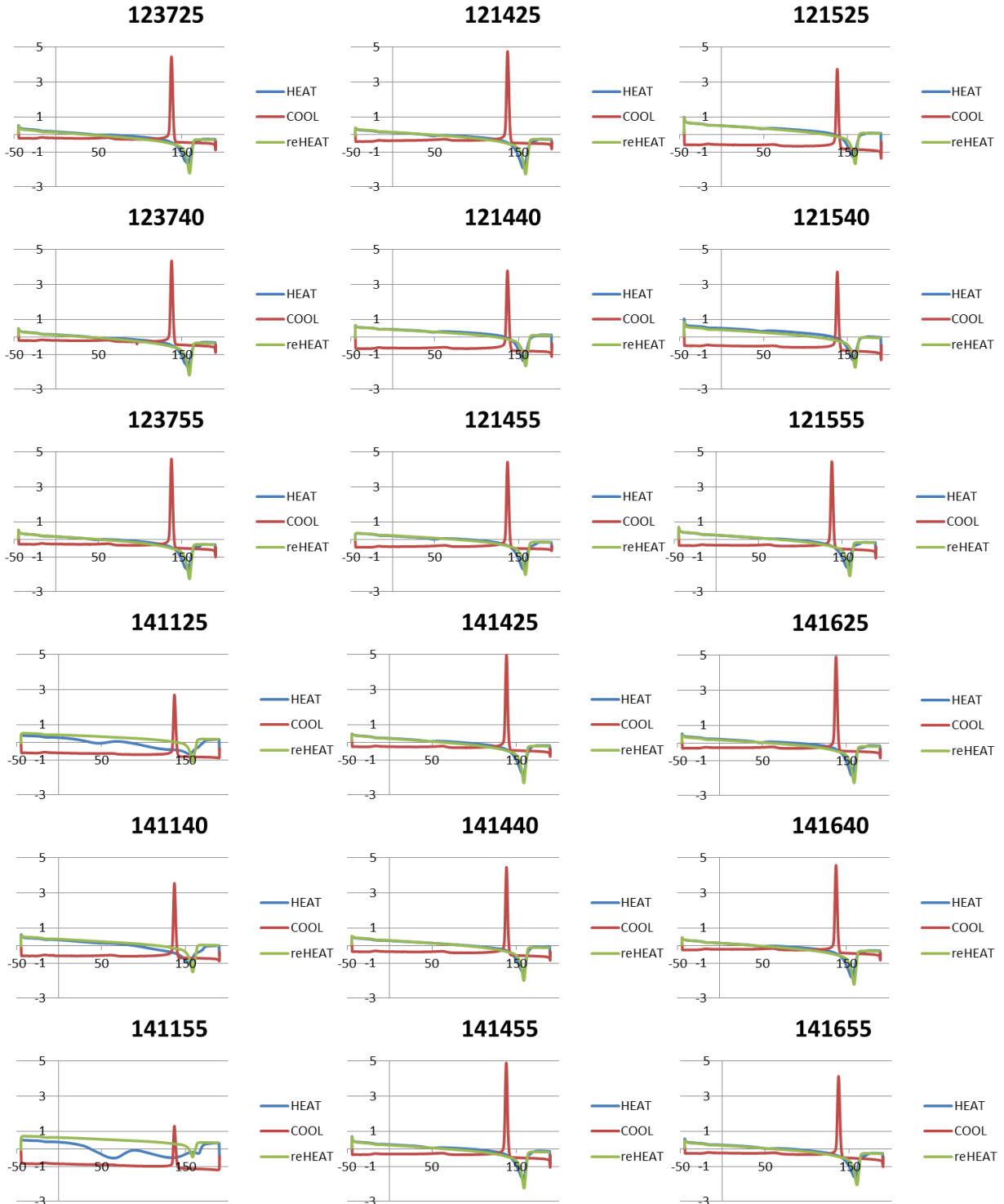
### FUTURE WORK

Since the fit model predicted only 30% of  $\beta$  crystallinity depending on three variables and their connected effects. More data from the experiment will help to see more precise trend. Although some conditions lead to higher  $\beta$  crystallinity compared to other samples using electrospinning process, some literatures suggest that higher  $\beta$  crystallinity can be obtained using other process. Post treatment such as annealing under tension on spun fibers might increase the  $\beta$  crystallinity even more as thermal effect increase crystallinity and stress applied orients the fiber. If carbon nanotube is added to the solution before electrospinning, the fibers will have increased strain-sensing ability because CNT will improve the alignment of dipole moment in piezoelectric material. Finally, measuring piezoelectricity to ensure that fibers with higher  $\beta$  crystallinity actually do possess higher piezoelectricity will be essential task.

APPENDIX A:

DSC DATA OF ELECTROSPUN PVDF FIBERS

OOOOOO: OO-wt%PVDF, O-DMAc to O-Acetone ratio, OO-Spinning Temperature(°C)

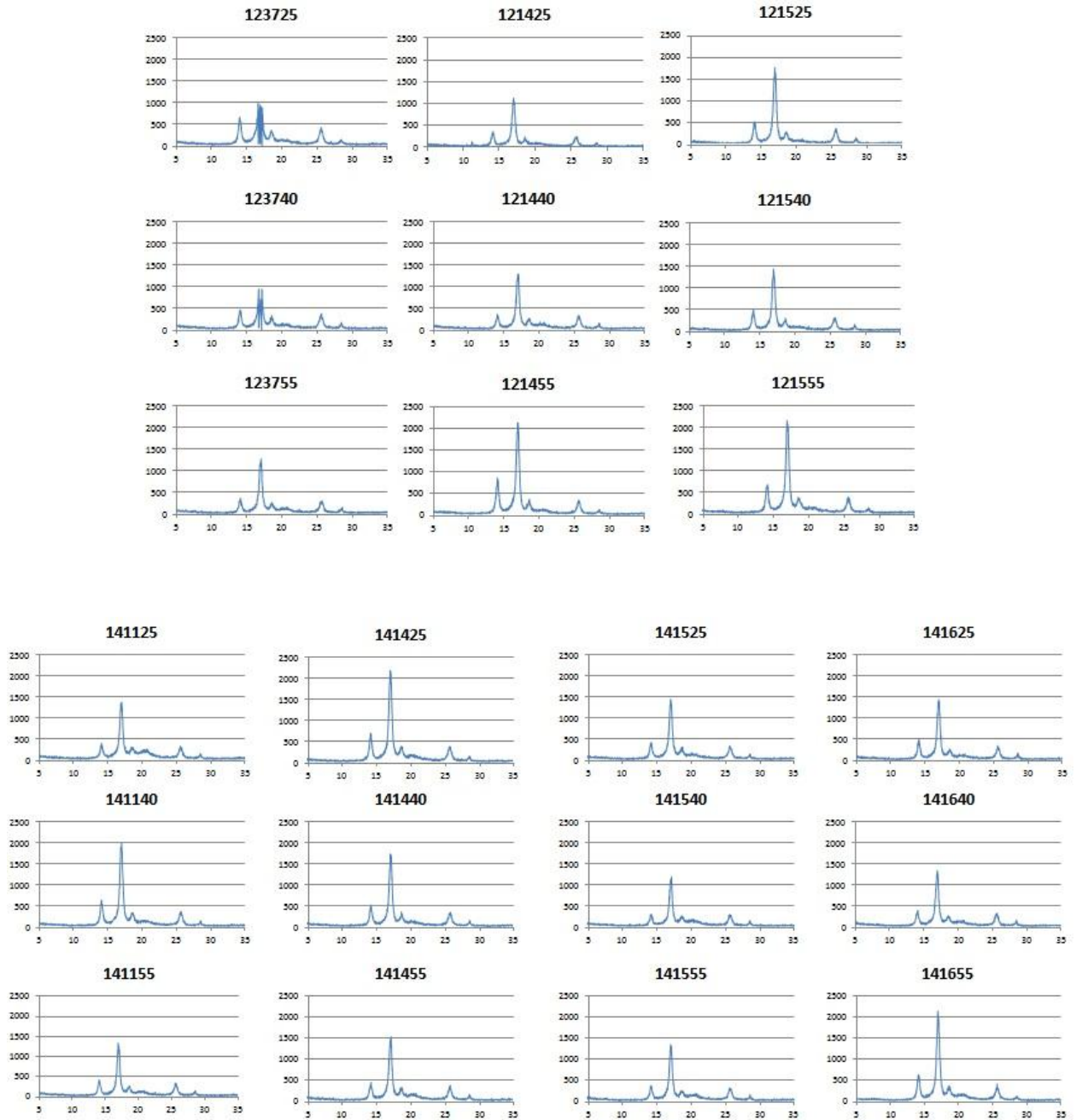


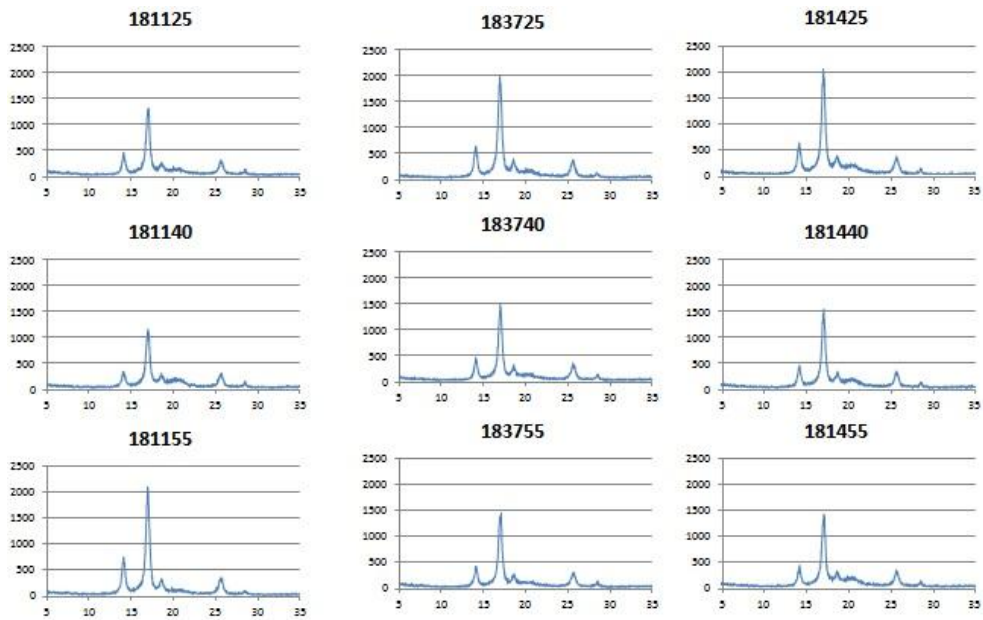
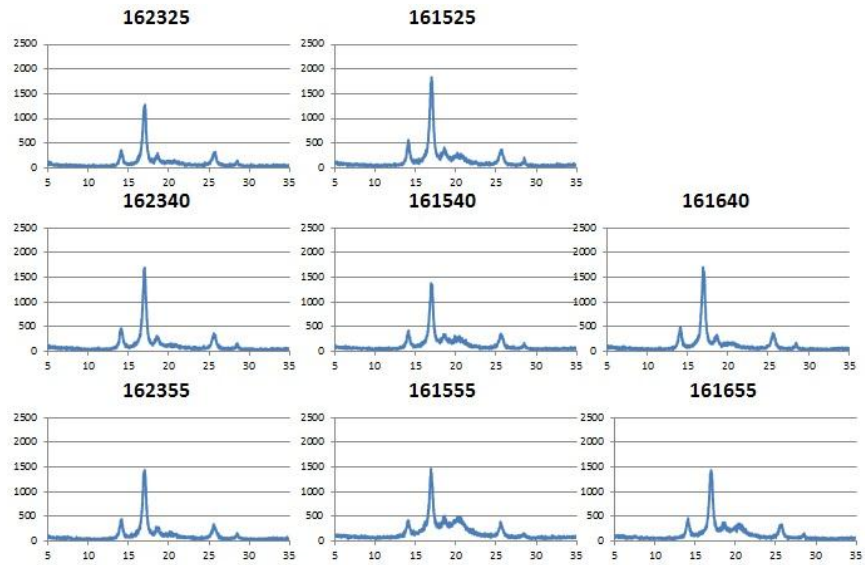


## APPENDIX B:

### XRD DATA OF ELECTROSPUN PVDF FIBERS

OOOOOO: OO-wt% PVDF, O-DMAc to O-Acetone ratio, OO-Spinning Temperature(°C)





## REFERENCES

1. Jungnickel B-. PVDF and its blends. PLASTICS ENGINEERING -NEW YORK- 1995;28:233.
2. Kim GH, Hong SM, Seo Y. Piezoelectric properties of poly(vinylidene fluoride) and carbon nanotube blends:  $\beta$ -phase development. Physical Chemistry Chemical Physics (Incorporating Faraday Transactions) 2009;11(44):10506-12.
3. Tashiro K. Crystal structure and phase transition of PVDF and related copolymers. PLASTICS ENGINEERING NEW YORK- 1995;28:63-.
4. Gautschi G. Piezoelectric sensorics : Force, strain, pressure, acceleration and acoustic emission sensors, materials and amplifiers. Berlin; New York: Springer; 2002. ID: 47785674.
5. Birlikseven C, Altintas E, Zafer Durusoy H. A low-temperature pyroelectric study of PVDF thick films. J Mater Sci : Mater Electron 2001;12(10):601-3.
6. Kawai H. The piezoelectricity of polyvinylidene fluoride 1969;8:975. Journal of Applied Physics 1969;8:975.
7. Kepler RG. Ferroelectric, pyroelectric, and piezoelectric properties of poly(vinylidene fluoride). PLASTICS ENGINEERING -NEW YORK- 1995;28:183.
8. Surface Characterization of polyvinylidene fluoride (pvdf) in its application as an actuator [Internet]College Station, Tex.: Texas A&M University; c2010.
9. Pauliat, Giles, Roosen, Gerald and Mathey. Influence of piezoelectricity on the photorefractive effect. Journal of the Optical Society of America 1991;8:1942.
10. Birkholz M. Crystal-field induced dipoles in heteropolar crystals II. Physical Significance: Physics B 1995(96):333.
11. Pantelis P. Properties and applications of piezoelectric polymers. Physics in Technology 1984;15:239.
12. Uchino K,. Ferroelectric devices. New York: Marcel Dekker; 2000. ID: 42888123.
13. glynne-jones p. Towards a piezoelectric vibration-powered microgenerator. Iee Proceedings Science Measurement and Technology 2001;148:68-72.

14. Costa LMM. Effect of solution concentration on the Electropray/Electrospinning transition and on the crystalline phase of PVDF. *MSA Materials Sciences and Applications* 2010;01(04):246-51.
15. Nasir M, Matsumoto H, Danno T, Minagawa M, Irisawa T, Shioya M, Tanioka A. Control of diameter, morphology, and structure of PVDF nanofiber fabricated by electropray deposition. *Journal of Polymer Science.Part B, Polymer Physics*. 2006;44(5):779.
16. Chinaglia DL, Gregorio R, Stefanello JC, Pisani Altafim RA, Wirges W, Wang F, Gerhard R. Influence of the solvent evaporation rate on the crystalline phases of solution-cast poly(vinylidene fluoride) films. *J Appl Polym Sci* 2010;116(2):785-91.
17. Yee WA, Kotaki M, Liu Y, Lu X. Morphology, polymorphism behavior and molecular orientation of electrospun poly(vinylidene fluoride) fibers. *Polymer* 2007;48(2):512-21.
18. Wannatong L, Sirivat A, Supaphol P. Effects of solvents on electrospun polymeric fibers: Preliminary study on polystyrene. *Polymer International*. 2004;53:1851-9.
19. Theron SA, Zussman E, Yarin AL. Experimental investigation of the governing parameters in the electrospinning of polymer solutions. *Polymer* 2004;45(6):2017-30.
20. Danno T, Matsumoto H, Nasir M, Shimizu S, Minagawa M, Kawaguchi J, Horibe H, Tanioka A. Fine structure of PVDF nanofiber fabricated by electropray deposition. *Journal of Polymer Science.Part B, Polymer Physics*. 2008;46(6):558.
21. Gregorio J, Rinaldo, Cestari M. Effect of crystallization temperature on the crystalline phase content and morphology of poly(vinylidene fluoride). *J.Polym.Sci.B Polym.Phys.Journal of Polymer Science Part B: Polymer Physics* 1994;32(5):859-70.
22. Ketpang K, Park JS. Electrospinning PVDF/PPy/MWCNTs conducting composites. *Synth Met* 2010;160(15-16):1603-8.
23. Thompson CJ, Chase GG, Yarin AL, Reneker DH. Effects of parameters on nanofiber diameter determined from electrospinning model. *Polymer* 2007;48(23):6913-22.
24. Fong H, Chun I, Reneker DH. Beaded nanofibers formed during electrospinning. *Polymer* 1999;40(16):4585-92.

25. Palade LI, Verney V, Attane P. Time-temperature superposition and linear viscoelasticity of polybutadienes. *Macromolecules* 1995;28(21):7051.